

# Holocene marine diatoms from the Faeroe Islands and their paleoceanographic implications

Ewa Witon<sup>a,\*</sup>, Björn Malmgren<sup>a</sup>, Andrzej Witkowski<sup>b</sup>, Antoon Kuijpers<sup>c</sup>

<sup>a</sup> Department of Earth Sciences–Marine Geology, Göteborg University, Box 460, SE-405 30 Göteborg, Sweden

<sup>b</sup> Department of Palaeoceanology, University of Szczecin, Waska 13, PL-71 415 Szczecin, Poland

<sup>c</sup> Geological Survey of Denmark and Greenland, Oster Voldgade 10, DK-1350 Copenhagen, Denmark

Received 17 June 2004; received in revised form 17 February 2006; accepted 21 February 2006

## Abstract

Temporal oceanographic changes based on mid- and late Holocene marine diatom floras from the Faeroe Islands region have been studied. The four studied coring sites are located in the Skalafjord and a more open-ocean environment, the mouth of the Kaldbaksfjord, at water depths ranging between 50 and 70 m. Comparison of the diatom records in the fjord sediments with those from the outer part of the fjord shows that the fjord provides a more optimum potential for paleoceanographic reconstructions. The concentrations of marine taxa and relative abundance of freshwater diatom species in the marine environment were analyzed with the aim of relating them to environmental conditions. Estimated diatom concentrations were very low and ranged from a maximum of  $14.4 \times 10^6$  valves per gram dry sediment in the inner part of the fjord to a minimum of  $0.1 \times 10^6$  outside the fjord. The freshwater diatom flora that occurred between 1200 and 700 cal. yr. BP in the inner part of the fjord suggests much higher precipitation during this time and increased freshwater discharge into the fjord. Presence of *Actinocyclus normanii*, which is an indicator of increasing trophicity, is related to the first human settlement on the Faeroe Islands. Maximum-likelihood factor analysis (MLFA) was used to describe the most essential relationship among the diatom species, and to employ these relationships for inferring Holocene environmental changes in the Faeroe Islands. The first two MLFA factors are related to oceanic influences in the region. Factor 1 is represented by a warmer water diatom assemblage and is suggested to correspond to inflow of the Norwegian–Atlantic Current to the Skalafjord, whereas Factor 2 is an indicator of a colder-water diatom assemblage that corresponds to inflow of Arctic–Norwegian Water Mixing (ANWM) during the 4900–3200 cal. yr. BP time interval.

© 2006 Elsevier B.V. All rights reserved.

**Keywords:** Faeroe Islands; Holocene; Marine diatoms; Relative abundances; Factor analysis

## 1. Introduction

Diatom assemblages in nearshore marine sediments have been used frequently as quantitative predictors of environmental parameters such as sea surface-water temperature (SST) (Jiang et al., 2002), salinity (Juggins, 1992), sea-level reconstruction (Zong and Horton, 1999;

Garcia-Rodriuez and Witkowski, 2003). The earliest publications dealing with marine and freshwater diatoms from the northern North Atlantic are from the nineteenth and early twentieth centuries (e.g., Lyngbye, 1819; Cleve, 1873; Lagerstedt, 1873; Cleve and Grunow, 1880; Østrup, 1895; Cleve, 1896; Østrup, 1897; Cleve, 1898, 1900; Gran, 1900; Brun, 1901). These publications were mostly devoted to taxonomic descriptions of the diatom floras from this region. Recently, marine diatoms of the North Atlantic have

\* Corresponding author.

E-mail address: [ewa.witon@wp.pl](mailto:ewa.witon@wp.pl) (E. Witon).

been used for studies of paleoclimatic and paleoceanographic changes following the last glacial period by Koç Karpuz and Schrader (1990), Koç Karpuz and Jansen (1992), Koç et al. (1993), Schrader et al. (1993a,b), Kohly (1998), and Jiang et al. (2001, 2002).

In this study, marine diatoms from Faeroe Islands fjord environments have been studied. The sensitive and unique environment within the Faeroese fjords offers the potential for high-resolution studies of marine climate variability along the coastal margins of the Faeroe Islands. Diatom assemblages found in this environment reflect offshore and near-shore processes, and their distribution is related to environmental variables such as sea-surface water temperatures (SST), nutrient conditions, eustatic sea-level changes, and coastal currents.

The Faeroe Islands, consisting of 18 large and small islands, are located in a uniquely sensitive part of the North Atlantic Ocean that is suitable for unravelling Quaternary climatic changes (Fig. 1). The Faeroe Islands are located in the midst of the northward flowing, warm Atlantic surface water (6–10 °C, salinity >35‰) and the cold Norwegian Sea Overflow Water that flows from the north along the bottom of the Faeroe Bank Channel and Faeroe Shetland Channel (Fig. 2). Thermohaline convection in the Norwegian–Greenland Seas generates the cold overflow water. The major water masses in the northern North Atlantic are Polar water (cold, <0 °C, and low salinity, 34‰, water) transported by the East Greenland Current, Arctic water (mixed water, slightly higher salinity ~35‰), and warmer, saline Atlantic waters advected by the North Atlantic

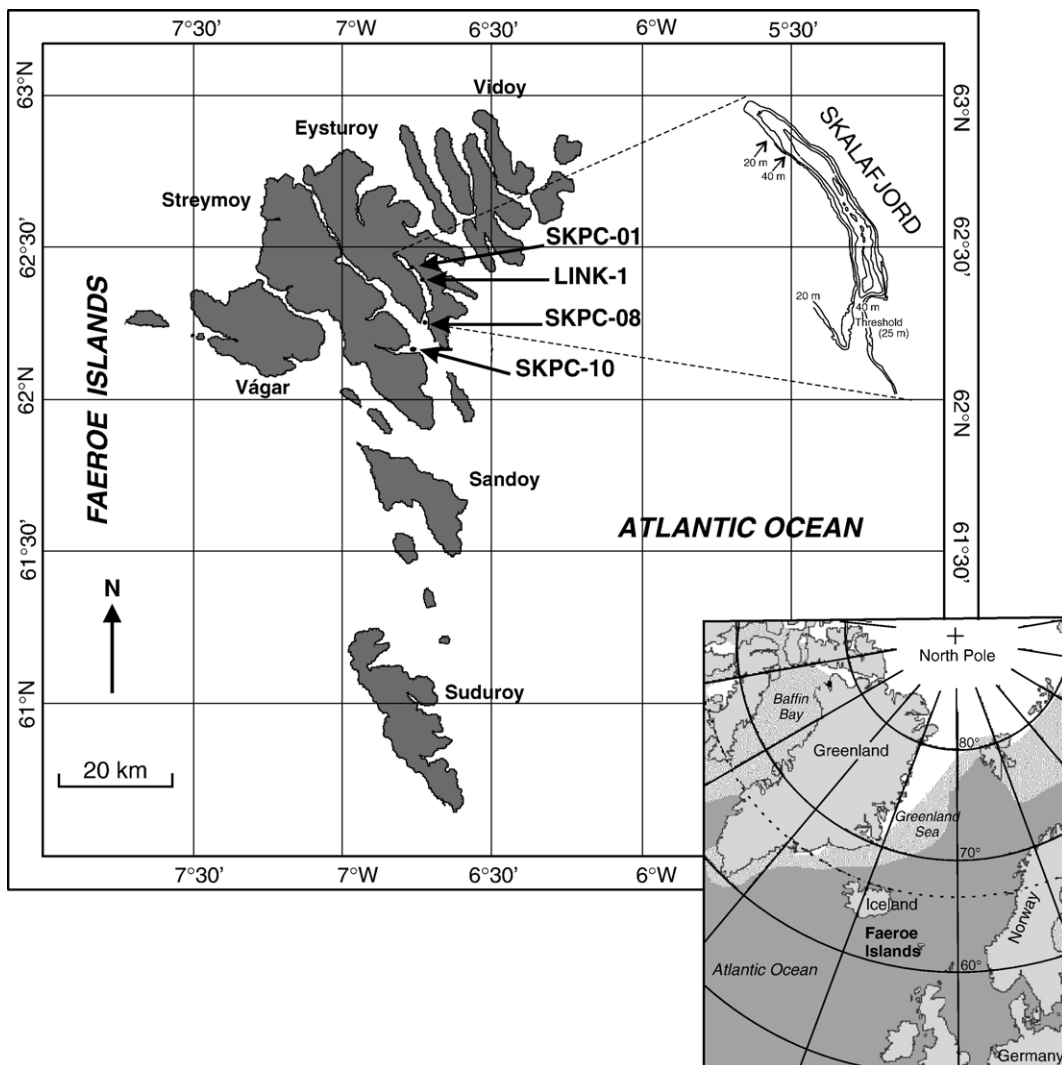


Fig. 1. Map of the Faeroe Islands showing the locations of the analyzed cores.

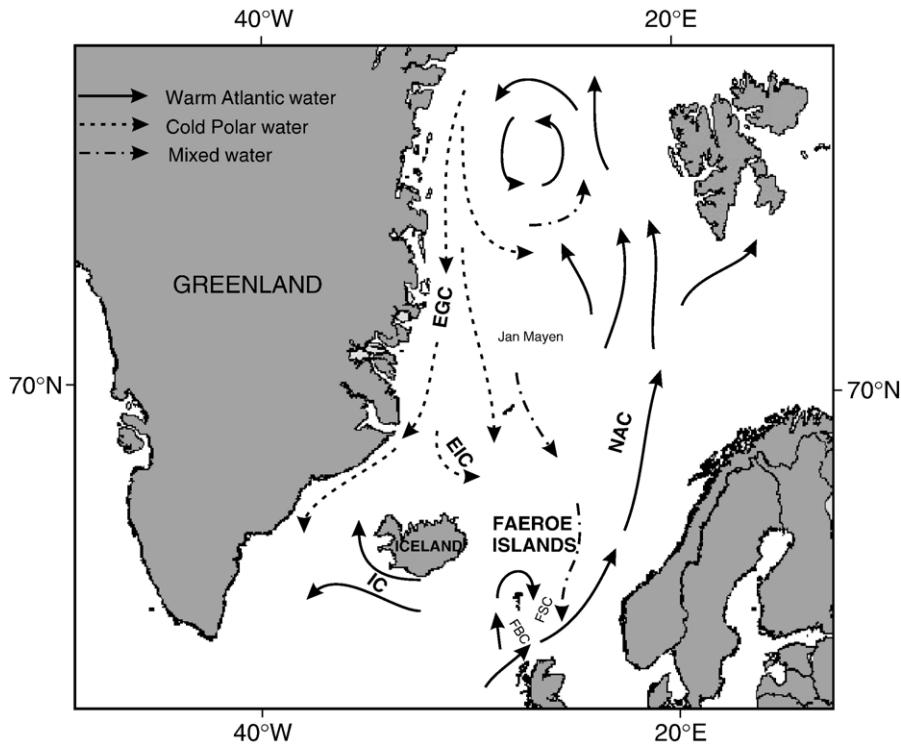


Fig. 2. Surface currents in the Greenland, Icelandic and Norwegian (GIN) Seas, and around the Faeroe Islands. EGC: East Greenland Current; EIC: East Iceland Current; NAC: North Atlantic Current; IC: Irminger Current; FSC: Faeroe–Shetland Channel; FBC: Faeroe Bank Channel.

Current (Hansen and Østerhus, 2000). The Faeroe Current, which is a part of the North Atlantic Current flows northward west of the Faeroe Islands (Hansen and Østerhus, 2000) and is relatively warm with SST in the range of 6–10 °C, and a bottom water temperature of about 6–7 °C with salinity range of 34–35‰.

One of the largest fjords in the Faeroe Islands is the Skalafjord (13 km long and with a maximum width of 1.5 km; maximum water depth of 70 m), from where the sediment cores analyzed here were retrieved. Seismic profiles show a thick Holocene sediment cover (15–20 m) in parts of the fjord (Larsen, 1991). Bottom-water circulation in the Skalafjord is characterized by low energy and stratified water masses (Hansen et al., 1990). During most of the year, the bottom waters of the fjord are characterized by low energy and oxygen content, and the water masses are stratified; occasionally, during some winters, the stratification is broken down (Hansen et al., 1990). Organic-rich waters derived from fishing, industrial outlets and sewage further reduce the oxygen level in the Skalafjord (Juil, 1992; Enell, 1996). Detailed accounts of the regional oceanographic setting of the Faeroe Islands and water mass circulation pattern are provided by Hansen et al. (1990) and Hansen and Østerhus (2000).

A number of studies carried out during the last ten-year period based, for example, on microfossil assemblages, including foraminifera (Rasmussen et al., 1996a, b), pollen (Hannon and Bradshaw, 2000), dinoflagellates (Roncaglia, 2004), and diatoms (Witon and Witkowski, 2003), tephra (Wastegård et al., 2001; Wastegård, 2002; Rasmussen et al., 2003), and sediments and sedimentation processes (Kuijpers et al., 1998a,b; Nielsen and van Weering, 1998; van Weering et al., 1998; Taylor et al., 2000; Kuijpers et al., 2002) have been instrumental for the understanding of past oceanographic conditions in the Faeroe Islands.

Koç Karpuz and Schrader (1990) defined six diatom assemblages by Q-mode factor analysis based on samples from the northern North Atlantic and correlated these assemblages with different water masses. Their study included samples from the northern North Atlantic area but did not include samples from the Faeroe Islands. To analyze diatom samples, especially the relationships among species through time, we employed MLFA rather than any Q-mode analysis.

The objectives of the present study are: (1) to describe the marine diatom floras and their concentrations in core sediments in the Faeroe Islands region; (2) to analyze the relative abundance of freshwater diatom

Table 1

Location and water depth of the piston cores from the Faeroe Islands, and the highest, the lowest, and average sedimentation rates for the cores

Core	Core length (cm)	Sampling date	Latitude	Longitude	Water depth (m)	Average sedimentation rate (mm/yr)	Highest sedimentation rate (mm/yr)	Lowest sedimentation rate (mm/yr)
LINK 01	1090	Aug. 2000	62°10.089 N	06°46.978 W	52	2.2	2.7	1.4
SKPC-01	220	Oct. 1995	62°10.707 N	06°47.870 W	50	0.3	0.4	0.2
SKPC-08	220	Oct. 1995	62°05.165 N	06°47.176 W	77	3.2	4.4	1.5
SKPC-10	240	Oct. 1995	62°02.895 N	06°45.033 W	74	3.6	4.0	0.3

species in the marine environment and discuss their implications for past environmental conditions; (3) to analyze the relative abundance of the marine diatom species and species groups, and temporal changes in these characteristics; (4) to compare these variables among cores retrieved from inside the fjord with cores from outside the fjord with a more open oceanic environment; (5) to determine the core chronology. Another goal of the study is to analyze the occurrence of local diatom assemblages in the Faeroe Islands using multivariate-statistical analysis and to interpret temporal fluctuations in these assemblages in terms of environmental change in this region.

## 2. Material and methods

### 2.1. Material

Four piston cores LINK-1, SKPC-01, SKPC-08, and SKPC-10, were analyzed in this study. The SKPC cores

were retrieved from the Faeroe Islands fjords during the September–October 1995 *R/V Skagerak* cruise organized by Göteborg University in collaboration with the Geological Survey of Denmark and Greenland (GEUS). The LINK-1 core was taken during the August 2000 *R/V Dana* cruise. The coring sites were situated in the Skalafjord and from the mouth of the Kaldbaksfjord at a water depth between 50 and 70 m (Fig. 1; Table 1).

Core LINK-1 was retrieved from the central part of the Skalafjord, and the coring site was located at a water depth of 52 m. The length of the core is 1090 cm, and it is characterized by predominantly homogeneous olive clayey mud (Fig. 3). Core SKPC-01 was also retrieved from the inner part of the Skalafjord. The core length is 220 cm, and the sediments are made up by predominantly homogeneous olive-grey clayey mud (Fig. 3). Core SKPC-10 was retrieved from a more open-ocean environment, namely from the mouth of the Kaldbaksfjord at a water depth of 74 m. The length of this core is 220 cm, and it is characterized by homogenous olive-

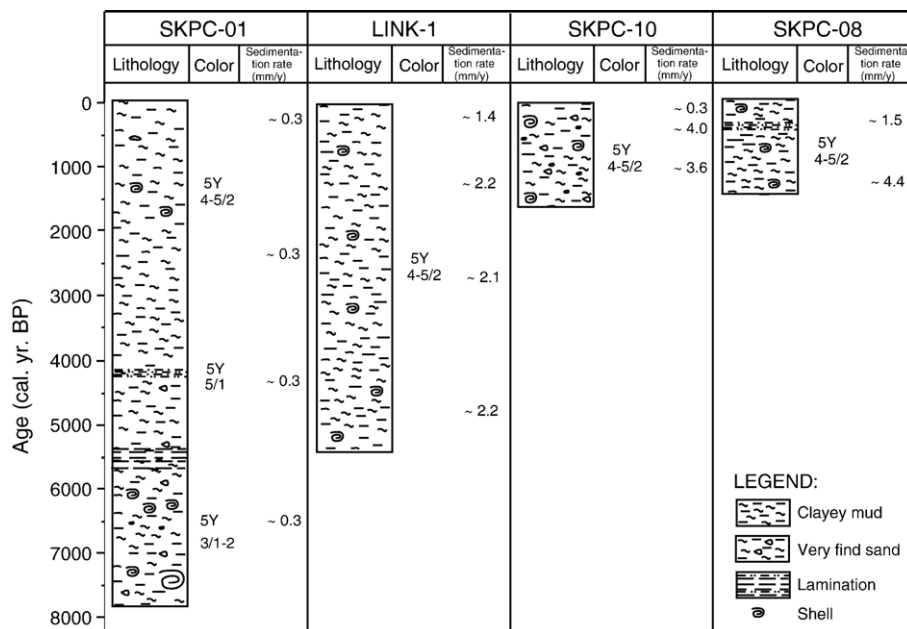


Fig. 3. Lithology and sedimentation rates for the cores.

grey very fine sand (Fig. 3). The preservation of diatoms was poor, as numerous valves were strongly fragmented or to a high degree affected by dissolution processes. Core SKPC-08 was taken from more open-ocean environments at the entrance to the Skalafjord at a water depth of 77 m. The length of the core amounted to 240 cm. The sediment studied was represented by homogenous olive-grey clayey mud (Fig. 3). The preservation of diatoms was similar to that of core SKPC-10 with numerous valves strongly fragmented or dissolved.

## 2.2. Sedimentation rates

Core SKPC-01, which is located in the innermost part of the Skalafjord, is characterized by the lowest sedimentation rate among the cores studied here; the sedimentation rate appears to be relatively constant at  $\sim 0.3$  mm/yr throughout the core (Table 1, Fig. 3). A lower sedimentation rate than in the other cores may be explained by the setting of the core site with respect to the prevailing (tidal) current and associated sediment transport pattern. In core LINK-1, located somewhat closer to the entrance of the Skalafjord, the sedimentation rate is considerably higher, being rather constant at  $\sim 2.2$  mm/yr, within the whole core profile. However, in the topmost part of the core it decreased to  $\sim 1.4$  mm/yr (Table 1, Fig. 3). In core SKPC-08, located at the entrance to the Skalafjord, the sedimentation rate was determined to be high, 4.4 mm/yr, at the bottom of the core (the interval dated to 1220–1460 cal. yr BP), and 1.5 mm/yr at the top of the core (between 1220 and 640 cal. yr BP) (Fig. 3). This high sedimentation rate was most likely induced by enhanced sediment input from a strong bottom current transport prevailing in this area. In core SKPC-10 a particular feature of the geological record was also a very high sedimentation rate,  $\sim 3.6$  mm/yr. (Table 1, Fig. 3), within the depth interval between 120 and 40 cm, which is dated at 1340–1120 cal. yr BP. This core, also located at the entrance to the fjord, is affected by the influence of bottom currents.

The chronology of the cores is based on fourteen radiocarbon AMS  $^{14}\text{C}$  analyses (Table 2) from macrofossil shells. The datings were performed at the University of Aarhus, Denmark and the Radiocarbon Laboratory of Poznan, Poland. Calibrated ages in calendar years were obtained from Stuiver et al. (1998) by means of the calibration program CALIB version 4.0 (Stuiver and Reimer, 1993). Reservoir corrected age were used in this study (cf. Table 2). Ages of certain levels were estimated through linear

Table 2

Results of AMS  $^{14}\text{C}$  dating of cores LINK-1, SKPC-01, SKPC-08, and SKPC-10

Core	Core depth (cm)	$^{14}\text{C}$ Age (BP)	Reservoir corrected $^{14}\text{C}$ age (BP)	Calibrated age $\pm 1\sigma$
LINK-1	69	1371 $\pm$ 43	971 $\pm$ 43	968 BP
LINK-1	285	2784 $\pm$ 37	2384 $\pm$ 37	2539 BP
LINK-1	472	3462 $\pm$ 37	3062 $\pm$ 37	3392 BP
LINK-1	703	4252 $\pm$ 47	3852 $\pm$ 47	4422 BP
LINK-1	949	4951 $\pm$ 48	4551 $\pm$ 48	5342 BP
SKPC-01	50	3380 $\pm$ 55	2980 $\pm$ 55	3260–3130 BP
SKPC-01	150	6235 $\pm$ 60	5835 $\pm$ 60	6710–6700 BP
SKPC-01	183	7465 $\pm$ 55	7065 $\pm$ 55	7980–7920 BP
SKPC-08	26	670 $\pm$ 25	270 $\pm$ 25	650–610 BP
SKPC-08	110	1310 $\pm$ 30	910 $\pm$ 30	1350–1220 BP
SKPC-08	215	1635 $\pm$ 25	835 $\pm$ 25	1660–1460 BP
SKPC-10	1	104.3 $\pm$ 0.2 pMC*	–	–
SKPC-10	40	1560 $\pm$ 60	1160 $\pm$ 60	1210–1030 BP
SKPC-10	120	1770 $\pm$ 70	1370 $\pm$ 70	1370–1310 BP

Used method: Method I, intercept ages (Stuiver et al., 1998).

\* Percent modern carbon.

interpolation between the AMS  $^{14}\text{C}$  dated levels assuming a constant sedimentation rate.

## 2.3. Methods

Samples were prepared following the procedure described by Håkansson and Ross (1984). Samples for diatom analyses were collected at 5 cm intervals in cores SKPC-01 and SKPC-08, at 1 cm intervals in core SKPC-10, and at 10 cm intervals in core LINK-1. Diatom analyses were performed with a LEICA DMLB light microscope, using a  $\times 100/1.25$  planapochromatic oil-immersion objective.

In each sample more than 300 valves were counted in transects for each sample (excluding *Chaetoceros* resting spores) using the counting procedure described by Schrader and Gersonde (1978). Relative abundances (percentages) of each species were computed in all samples.

Diatom identification was based on the work by Hasle (1978), Metzeltin and Witkowski (1996), and Witkowski et al. (2000). Diatoms were divided into groups according to their ecological requirements following Hasle and Syvertsen (1996) and Witkowski et al. (2000).

## 2.4. Statistical analysis

To describe the most essential relationship among the diatom species, and to employ these relationships for inferring Holocene environmental changes in the Faeroe

Islands, we used maximum-likelihood factor analysis (MLFA) which has during the last 20 years become the most widely implemented factor-analytical model in the Earth sciences. Since our primary interest was to analyze relationships among species through time we employed MLFA rather than any Q-mode analysis. MLFA has the advantage over other R-mode techniques, such as principal component analysis (PCA), in its orientation being towards the reproduction of the interrelationships (correlation coefficients) between pairs of species rather than the decomposition of the variance of the species as in PCA.

In order to establish a common scale of variability for all variables, we used the correlation matrix as the basis for the MLFA. In contrast to the standard multivariate ordination method of PCA, which is oriented towards the representation of a maximum portion of the variance of the variables in a minimum number of new variables (the principal components), the factor-analytical model is instead directed towards the reproduction of the interrelations (in this case the correlation coefficients) between pairs of variables in a minimum number of factors. Comprehensive descriptions of the MLFA model are provided by Lawley and Maxwell (1971) and Reyment and Jöreskog (1993). In order to obtain “simple structure” of the factor loadings, the initial orientations of the factor axes were subjected to an oblique rotation employing the promax solution described by Hendrickson and White (1964). The significance of the contribution of the respective variables to the promax-rotated factors was tested using 95% bootstrap  $BC_a$  confidence intervals (Efron and Tibshirami, 1993). The  $BC_a$  confidence interval is considered to represent a substantial improvement over other bootstrap confidence intervals, such as the percentile method (Efron and Tibshirami, 1993). We used 2000 bootstrap replication in the derivation of the 95% bootstrap  $BC_a$  confidence intervals. For computation of the oblique factor scores, we used the procedure introduced by Thomson (1951). Prior to the MLFA the relative abundance data were subjected to a log–ratio transformation to relieve the constant-sum constraint inherent in such data (Aitchison, 1986).

The MLFA was applied to core Link-1. The data set consisted of 110 samples and the 11 most abundant species. In order to exclude rare taxa whose presence in the analysis might confuse the inferences, only species that occur with a relative abundance of >4% in at least one sample were used in the MLFA. The MLFA thus did not include cores SKPC-01, SKPC-08, and SKPC-10, where the diatom

assemblages consist predominantly of *Paralia sulcata* (ca. 80–95%).

### 3. Results

#### 3.1. Occurrence of freshwater diatoms in the marine environment

The diatom flora is almost exclusively marine in all cores, although freshwater species appear as well. The relative abundance of freshwater diatoms ranges between 0 and 7.9% (Fig. 4). The highest abundance (7.9%) occurs in lowermost part of the core SKPC-01 and the age of this section is 6900 cal. yr BP (Witon and Witkowski, 2003). After the marine environment had been established (after 6900 cal. yr BP), freshwater species still show increased abundances especially between 5300 and 4700 cal. yr BP and at 2300 cal. yr BP (2.8–2.1% and 3.5%, respectively; Fig. 4). Core LINK-1 also retrieved from inside the Skalfjord does not penetrate the strata containing the lacustrine environment signature. It therefore does not show a strong influence of a freshwater flora, the highest peak (6%) occurs at 850 cal. yr BP. Although cores SKPC-10 and SKPC-08 were retrieved from more open-ocean environments (Fig. 1) freshwater floras were identified there as well. In core SKPC-10 the highest influence (0.8–6.3%) were found in the time interval 1200–0 cal. yr BP and in SKPC-08 a somewhat higher relative abundance of freshwater diatoms (2.3–4.0%) was found in the time interval 1100–1300 cal yr BP.

#### 3.2. Concentration of marine diatoms

Diatom concentrations in cores LINK-1 and SKPC-01, which are located inside the fjord in a less dynamic environment that is more favourable for high standing stocks of diatoms, are, as expected, greater than in the region outside the fjords from where core SKPC-10 and SKPC-08 were retrieved.

##### 3.2.1. LINK-1

This core is characterized by the highest diatom concentration among the cores analyzed. In the lowermost interval of the core (1090–1000 cm) concentration is low ( $3.3\text{--}1.5 \times 10^6$  valves/g sed.) and the maximum absolute abundance ( $14.4 \times 10^6$  valves/g sed.) attain at 4300 cal. yr BP (Fig. 5). After that time diatom concentration decreased gradually from  $3\text{--}6 \times 10^6$  to  $1.4 \times 10^6$  valves/g sed., although around 700 cal. yr BP there was a small increase.

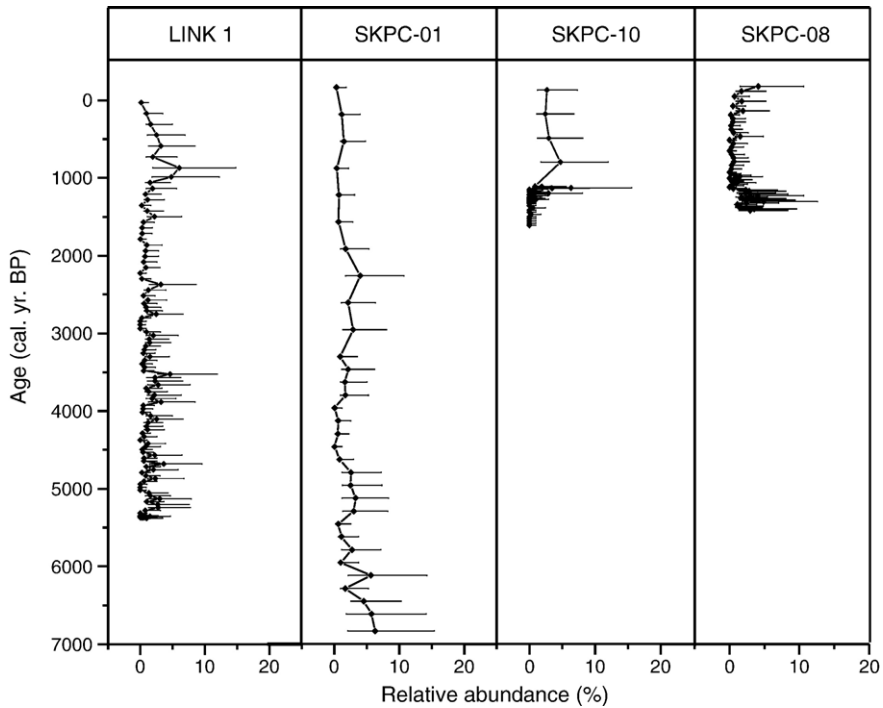


Fig. 4. Changes in the relative abundance of freshwater diatoms in the four examined cores. Horizontal bars represent 95% confidence interval for the relative abundances.

3.2.2. *SKPC-01*

In this core the absolute abundance pattern is similar to that in LINK-1. Two peaks of high absolute

abundance occur, the first one at around 5800 cal. yr BP ( $9.1 \times 10^6$  valves/g sed.) and the second one 700 years later at 5100 cal. yr BP ( $9.2 \times 10^6$  valves/g

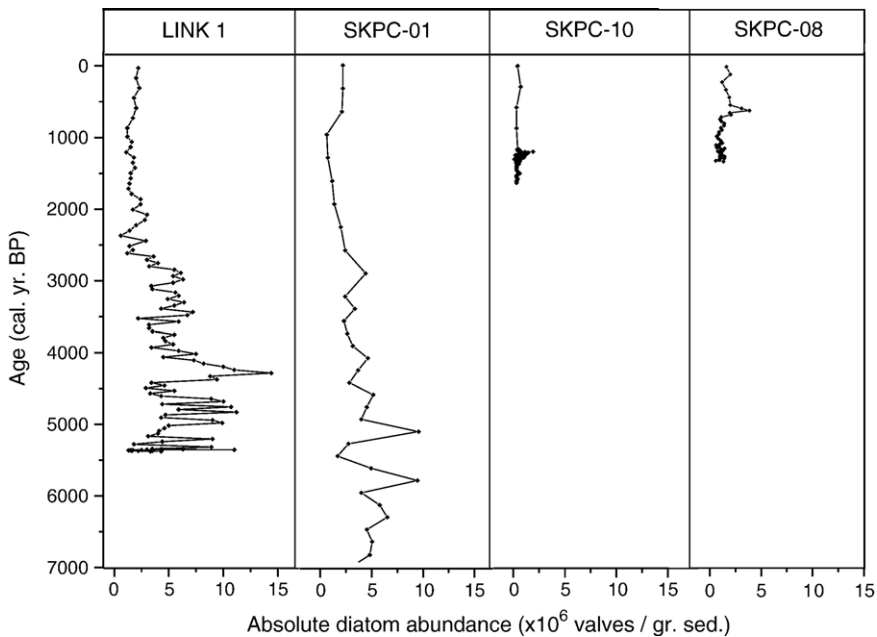


Fig. 5. Changes in the concentration (number of diatom valves per 1 g of dry sediment) of marine diatoms in the analyzed cores.

sed.). After that time diatom valves concentration decreased to  $0.7 \times 10^6$  valves/g sed. at 1000 cal. yr BP (Fig. 5).

### 3.2.3. SKPC-10

The lowest diatom concentration was observed in this core. Values here are relatively constant in ranging between  $0.3$  and  $0.5 \times 10^6$  valves/g sed. A small increase ( $1.9 \times 10^6$  valves/g sed.) is recorded in the lower part of the core between 1200 and 1100 cal. yr BP (Fig. 5).

### 3.2.4. SKPC-08

This core is also characterized by low diatom concentrations. They were relatively constant between  $0.9 \times 10^6$  and  $1.1 \times 10^6$  valves/g sed., except for an increase to  $4.1 \times 10^6$  valves/g sed. in the upper part between 700 and 600 cal. yr BP (Fig. 5).

## 3.3. General pattern of fluctuation in species composition

Totally 179 diatom taxa were identified in all four cores. The identified taxa are listed in Appendix A. In general, the state of preservation of the diatom valves was satisfactory. However, in cores located outside the fjords, valves were strongly fragmented. In most of the studied cores, three local diatom assemblage zones (DAZ), were distinguished. Changes in diatom concentration, species composition, and diatom ecological groups (freshwater, brackish, and marine) were applied as criteria to distinguish the DAZ.

### 3.3.1. LINK-1

In this core three diatom assemblage zones were distinguished (Fig. 6):

**3.3.1.1. DAZ-1a (5400–4000 cal. yr BP).** The upper limit of DAZ-1a is marked by the disappearance of *Rhizosolenia hebetata*. In general, this zone is characterized by high relative abundance of *P. sulcata* (up to 73%), *Thalassiosira angulata* (up to 40%), *Thalassionema nitzschioides* (up to 30%), *R. hebetata* (up to 26%), and *Odontella aurita* (up to 21%). Within this part of the core percentages of planktonic taxa exceeded 70%.

**3.3.1.2. DAZ-2a (4000–2600 cal. yr BP).** The distinguishing criteria for DAZ-2a were the highest diatom concentration (up to  $14.4 \times 10^6$ ; Fig. 5) and the highest number of diatom species noted in all four cores. One of the most characteristic features of this

zone is the increase in *Cocconeis costata*, *Dimeregramma fulvum*, *Grammatophora angulosa* var. *islandica*, and *Rhabdonema minutum*, which from a habitat point of view represent epiphytic forms, usually growing attached to macrophytes (Kuylenstierna, 1989–1990; Snoeijis, 1994; Witkowski, unpublished observations).

**3.3.1.3. AZ-3a (2600–0 cal. yr BP).** The diatom assemblage of this zone is predominantly composed of benthic species. Its lower limit is marked by distinct decreases in *O. aurita*, *T. angulata*, and *T. nitzschioides*. Simultaneous indistinct increases in *Navicula distans* and *G. angulosa* var. *islandica* are observed as well. *P. sulcata* reaches its maximum relative abundance (89%) in this zone.

### 3.3.2. Core SKPC-01

Three local diatom assemblage zones were distinguished in this core (Fig. 7).

**3.3.2.1. DAZ-1b (7700–6500 cal. yr BP).** This DAZ is characterized by high relative abundance of *O. aurita* (up to 27%), *T. nordenskiöldii* (up to 18%), *Thalassiosira decipiens* (up to 16%), and *P. sulcata*, whose relative abundance continuously increased from 0% to 71%. Some of the taxa, like *T. decipiens*, *G. angulosa* var. *islandica*, *T. nitzschioides*, and *C. costata*, reach their maximum abundance in this zone but did not exceed 8%.

**3.3.2.2. DAZ-2b (6500–2600 cal. yr BP).** This zone is characterized by a completely different species distribution pattern when compared to the preceding one. It is noteworthy that some abundant species (e.g., *T. decipiens*, *G. marina*, *R. minutum*, and *Actinopteryx senarius*) are characterized by a discontinuous core distribution. Distinct increases in abundance of *P. sulcata*, *N. distans*, *R. minutum*, *R. hebetata*, *A. senarius*, and *T. nitzschioides* in the middle part of the zone.

**3.3.2.3. DAZ-3b (2600–0 cal. yr BP).** In DAZ-3b most of the species disappeared. *P. sulcata* reached the maximum in this zone. Through the zone this species constituted up to 93% of the whole diatom assemblage. A group of taxa that shows increased abundance in this section: *G. angulosa* var. *islandica*, *N. distans*, *D. fulvum*, and *A. senarius*. *A. senarius* reached its maximum relative abundance (3%) in the upper part, where the other species, except *P. sulcata* and *C. costata*, were gradually disappearing.

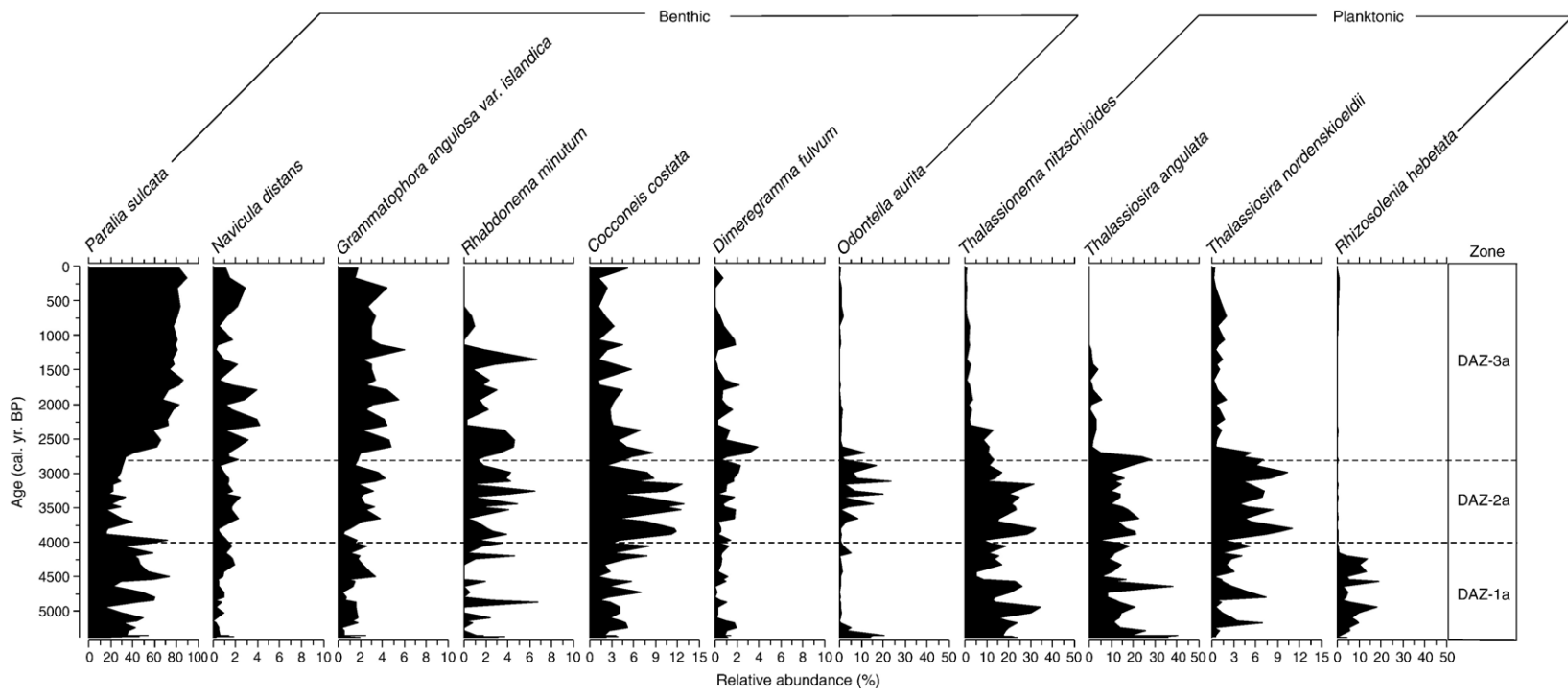


Fig. 6. Fluctuations in the relative abundance of the most common marine diatom taxa in core LINK-1.

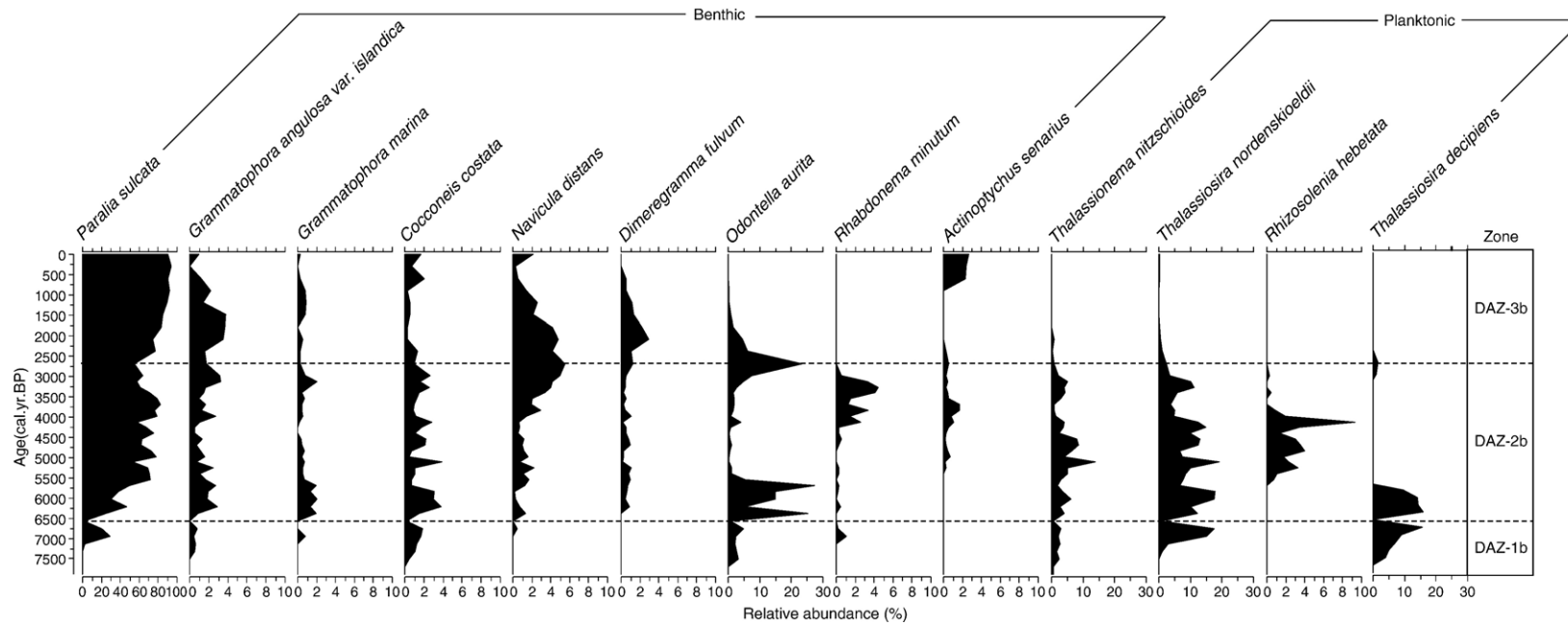


Fig. 7. Fluctuations in the relative abundance of the most common marine diatom taxa in core SKPC-01.

### 3.3.3. Core SKPC-10

In this core two local diatom assemblage zones were distinguished (Fig. 8).

**3.3.3.1. DAZ-1c (1630–1250 cal. yr BP).** The diatom assemblage of this zone is dominated by the tycho-planktonic species *P. sulcata* (88–97%). In addition, a few other species were identified, including for example, epipellic (e.g., *A. senarius*, up to 6%), planktonic (e.g., *T. nordenskiöldii*, up to 5%), and epiphytic (e.g., *G. angulosa* var. *islandica*, up to 3%) forms. Their patterns of distribution are very similar along the whole zone profile.

**3.3.3.2. DAZ-2c (1250–0 cal. yr BP).** This DAZ, marked by distinctly lower sedimentation rate (Table 1, Fig. 3), is characterized by much higher diversity of the diatom flora. The content of the dominant species, i.e., *P. sulcata*, shows a gradual upward decrease from 90% to 41%. The benthic forms show a distinct decrease in the middle part of the zone. In this part of the core they were replaced by all planktonic forms that appeared first in this part of the zone. The only exception to this tendency amongst the benthic taxa was *C. costata*, which appeared first in this part of DAZ-2c and gradually increased to up to 7%.

### 3.3.4. Core SKPC-08

The distribution pattern of the diatom flora is rather consistent throughout the core with low variation in species composition. Based on the distribution of species three local diatom assemblage zones were distinguished (Fig. 9):

**3.3.4.1. DAZ-1d (1500–1350 cal. yr BP).** The diatom assemblage of this zone is strongly dominated by *P. sulcata* (up to 89%). The most abundant of them (less than 5%) were *G. angulosa* var. *islandica*, *C. costata*, and *D. fulvum* (benthic forms), and *Actinocyclus normanii*, *T. nordenskiöldii*, and *T. nitzschioides* (planktonic species).

**3.3.4.2. DAZ-2d (1350–800 cal. yr BP).** The beginning of this zone is marked by the appearance of *N. distans* (up to 4%). The abundances of the remaining species show more or less the same range of magnitude and distribution pattern as in DAZ-1d.

**3.3.4.3. DAZ-3d (800–0 cal. yr BP).** The lower boundary of this zone is marked by the appearance of the benthic species *A. senarius* (up to 7%). Planktonic species abundance is less than 4%, while

the hitherto dominating *P. sulcata* shows a gradual upward decrease to 76%. The remaining species show a distribution pattern similar to that in the previous two zones. Noteworthy is, however, a distinct peak of *A. normanii* in the uppermost part of the core.

### 3.4. Maximum-likelihood factor analysis (MLFA)

The MLFA was applied to core LINK-1 using a log-ratio transformation of the percentage data. From the total number of species (46) from this core we used the 11 most abundant species as input variables to the MLFA in order to provide evidence of the major fluctuations in the diatom flora. Two factors were found to represent the optimum solution based on inspections of the residual correlation matrix (portion of correlations not reproduced by the factor model). The factor loadings of the species along these two factors are displayed in Table 3.

Even if the major idea behind MLFA is not to maximize the variability in the data-set in a minimum number of new variables as in principal component analysis but to reduce the correlation structure of the data, it may be mentioned that the total variability accounted for by these two factors is 43.9%.

#### 3.4.1. Factor 1

The fluctuations in the promax factor scores for this factor (Fig. 10, left panel) show high scores in the interval between the bottom of the core (5400 cal. yr BP) and about 1700 cal. yr BP, but in this interval a small decrease is recorded between 4900 and 3200 cal. yr BP. From 1700 cal. yr BP and the top of the core the scores decrease gradually. The higher scores during the time period 5400–1700 cal. yr BP indicate a high relative abundance of *T. nitzschioides* and *T. angulata* (species with positive factor loadings), and low relative abundance of *P. sulcata*, *N. distans*, and *G. angulosa* var. *islandica* (species with negative loadings) in this interval. In the topmost part of the core (subsequent to 1700 cal. yr BP), the relative abundance of *P. sulcata*, *N. distans*, and *G. angulosa* var. *islandica* increased gradually at the expense of *T. nitzschioides* and *T. angulata*.

Species with a positive factor loadings (*T. nitzschioides* and *T. angulata*) are planktonic and species with a negative factor loadings (*P. sulcata*, *N. distans* and *G. angulosa* var. *islandica*) are benthic. *P. sulcata*, the third species with a negative factor loadings may be either benthic or tycho-planktonic. However, this association with benthic taxa suggest

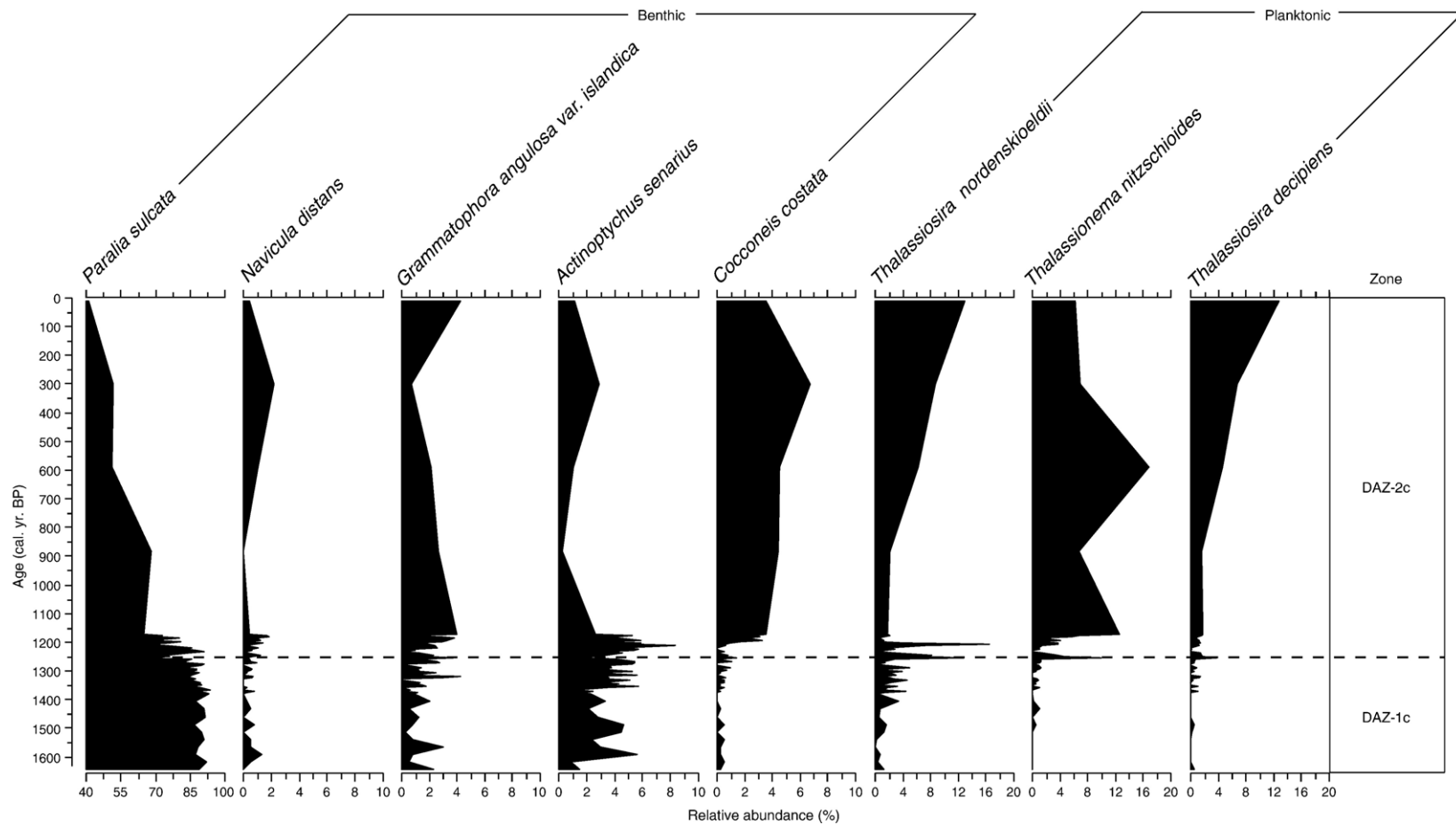


Fig. 8. Fluctuations in the relative abundance of the most common marine diatom taxa in core SKPC-10.

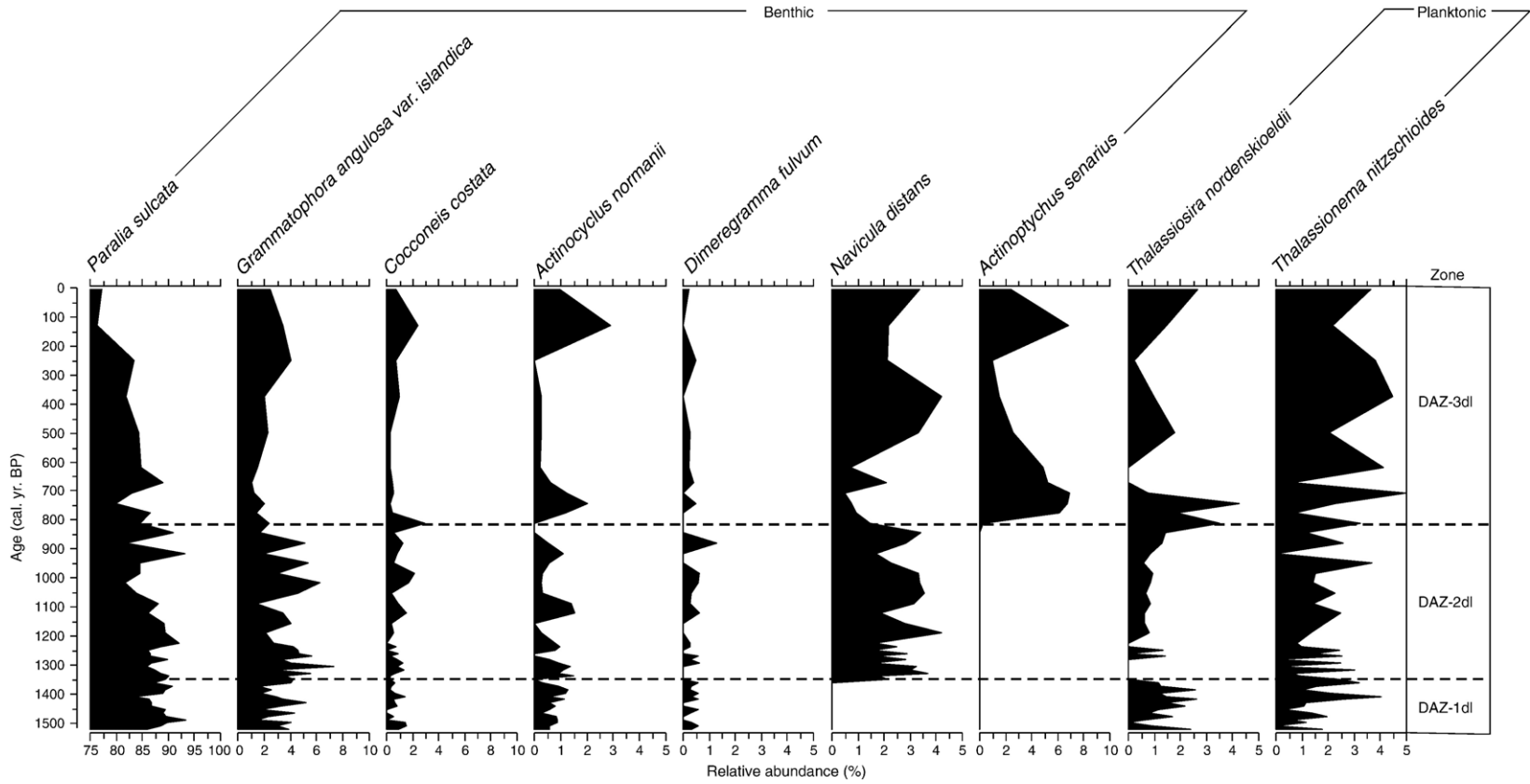


Fig. 9. Fluctuations in the relative abundance of the most common marine diatom taxa in core SKPC-08.

Table 3

Promax-rotated factor loadings for the 11 species used in maximum-likelihood factor analysis of core LINK-1 and 95% bootstrap  $BC_a$  confidence intervals for the loadings

Species	Factor 1			Factor 2		
	Loadings	Confidence interval		Loadings	Confidence interval	
<i>Cocconeis costata</i>	-0.4159	-0.7582	0.0813	-0.2122	0.9602	0.3488
<i>Dimeregramma fulvum</i>	0.0199	-0.3057	0.3068	-0.3248	-0.7777	0.2331
<i>Grammatophora angulosa</i> var. <i>islandica</i>	<b>-0.8324</b>	-0.9647	-0.1722	-0.1066	-0.8748	0.2388
<i>Navicula distans</i>	<b>-0.6148</b>	-0.7863	-0.1537	-0.1610	-0.7153	0.2671
<i>Odontella aurita</i>	0.3354	-0.0814	0.7370	-0.2941	-1.0121	0.2445
<i>Paralia sulcata</i>	<b>-0.8753</b>	-1.0855	-0.0723	0.1719	-0.8184	0.4191
<i>Rhabdonema minutum</i>	0.1571	-0.3863	0.4365	<b>-0.5611</b>	-1.0563	-0.0990
<i>Rhizosolenia hebetata</i>	0.0590	-0.1850	0.3201	<b>0.9845</b>	0.2807	1.0758
<i>Thalassionema nitzschioides</i>	<b>0.5630</b>	0.0541	1.0143	0.1575	-0.3211	0.7681
<i>Thalassiosira nordenskiöldii</i>	-0.2315	-0.7841	0.2411	-0.1505	-1.0757	0.5096
<i>Thalassiosira angulata</i>	<b>0.7992</b>	0.5234	0.9345	-0.0698	-0.6280	0.2760

The loadings that do not intercept a zero value are interpreted as significant (marked in bold).

that it may be preferentially a benthic species in the Skalafjord.

#### 3.4.2. Factor 2

The fluctuations in the promax factor scores for the second factor (Fig. 10, right panel) show high scores in the interval between 4900 and 3200 cal. yr BP. Then from 3200 to 1700 cal. yr BP the scores decrease, but some intervals with higher scores are apparent in this time interval. From 1700 cal. yr BP and the top of the core the scores gradually increased. The higher scores during the time period 4900–3200 cal. yr BP indicate a high relative abundance of *R. hebetata* (species with positive factor loadings), and low relative abundance of *R. minutum* (species with negative loadings) in this interval. In the rest of the core (from 3200 cal. yr BP to the top of the core), *R. hebetata*, which is a planktonic species, almost disappeared, and the relative abundance of the benthic species *R. minutum* increased instead.

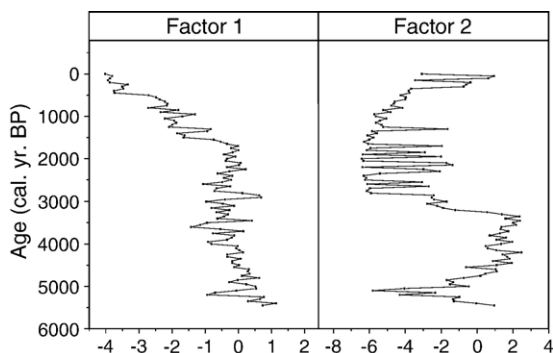


Fig. 10. Variation in scores of the first and second promax factors in Link-1.

## 4. Discussion

There are rather few reports in the literature on diatom-based paleoclimatic reconstructions in the North Atlantic. The diatom sedimentary record from the North Atlantic has been mostly used for paleocirculation reconstruction (e.g., Koç Karpuz and Schrader, 1990; Koç Karpuz and Jansen, 1992; Koç et al., 1993; Birks and Koc, 2002; Witak et al., 2005). This is in contrast to studies in the North Atlantic region based on other proxies, which have been successfully applied for paleoclimatic reconstructions (e.g., Calvo et al., 2002; Risebrobakken et al., 2003; Andrews and Giraudeau, 2003; Moros et al., 2004).

With the acknowledgments of the problems with the diatom record in the North Atlantic we have aimed at exploring the sediments of sheltered areas, like the fjords, in the Faeroe Islands, the records of which are related to the general circulation pattern of the area. This study indicates that the Skalafjord provided a favourable depositional environment for diatoms preservation during the mid- and late Holocene. The sediment cores retrieved from this fjord indicate a calm environment with lower sedimentation rates ( $\sim 0.3$ – $2.2$  mm/yr). This is quite opposite to the sediments from the outer part of the fjord, which were deposited in a highly dynamic, turbulent environment. Estimated sedimentation rates outside the fjord ( $\sim 3.6$  mm/yr) are much higher than those recorded in the interior of the fjord (Table 1; Fig. 3). Bottom currents at the mouth of the fjord are much stronger and play a major role in transportation and redeposition of diatom valves.

Estimated diatom concentrations in the study area ranged from a maximum of  $14.4 \times 10^6$  valves per gram of dry sediment from the inner part of the fjord (core LINK-

1) to a minimum of  $0.1 \times 10^6$  valves per gram of dry sediment in core SKPC-10 located outside the fjord (Fig. 5). Also the higher concentrations in the Skalafjord interior are very low in comparison to the Chukchi Sea (Polyakova, 1994), the North Atlantic and Nordic Seas where concentrations may be as high as  $83.0 \times 10^6$  valves per gram of dry sediment (Koç Karpuz and Schrader, 1990). Diatom abundance similar to those in the Faeroe Islands fjords ( $0.01$ – $6.7 \times 10^6$  valves per gram of dry sediment) has been found in sediments from the Laptev Sea (Cremer, 1999). The reason for these low valve concentrations is most likely due to lateral transport processes, pronounced dissolution, and low productivity in the euphotic zone in relation to relatively stable water mass stratification.

The most dominant taxon was *P. sulcata*, which is a common member of neritic diatom populations. Its contents in our cores are very high and reach up to 98% (Fig. 8). This species may be enriched through sorting processes on the sea-floor, because it has a robust frustule that withstands transport and dissolution well (Schrader et al., 1993b). In the outer part of the fjords the accumulation of this species can be attributed to a sorting and transport effect on the sea-floor, because at the bottom strong dynamic processes are prevalent. Only the very robust species persist and a great deal of the delicate marine planktonic diatom frustules is broken or dissolved. Much more favourable conditions for diatom valve preservation within the sediment are recorded in the inner part of the Skalafjord. Absolute abundance of diatoms was higher and preservation state was satisfactory. *P. sulcata* still is a dominant species, but a much higher diversity marks diatom assemblage within the Skalafjord than in the cores from outside the fjord. However, in the case of the cores taken outside of the fjord this may partly be a result of redeposition and enrichment of the sediment by lateral transport. In our interpretation, small size of *Thalassiosira* spp. which usually have a slightly silicified frustule, were removed, whereas the abundances of *P. sulcata* and other heavy taxa were enhanced. Another species subject to such a process might be *A. senarius*. The mechanisms behind an enrichment of *P. sulcata* were pointed out already by Schrader et al. (1993b). A certain role in an enrichment of fossil diatom assemblages may also be played by dissolution (e.g., Schrader, 1972; Baldauf, 1981). However, in such a dynamic system as the one prevalent at the mouth of the Skalafjord, the extent of dissolution seems to play a minor role. The disturbed diatom record is best illustrated in the lower and middle parts of core SKPC-10, where the dominance of *P. sulcata* in some samples exceeds 95% (Fig. 8). In the uppermost part of

this core the diatom record seems to represent the natural distribution. This is evidenced by a strong decrease of *P. sulcata* and appearance of other taxa that are not present in the lower parts of the core. *P. sulcata* can be either benthic or planktonic species and need constant wind to be kept in the water column at good light condition. Wind also has to be taken in consideration as one of the factors responsible for vertical and lateral transport.

The second feature in common for the cores studied is a distinct mixture of benthic taxa. This feature is again less pronounced in core SKPC-10, where benthic taxa are much less abundant than in the remaining cores. Abundant occurrence of the benthic and epiphytic taxa is quite understandable as the cores were taken from shallow water depths. The proportions of benthic taxa to *P. sulcata* and to planktonic taxa, e.g., *Thalassiosira* spp., *T. nitzschioides*, *R. hebetata*, and *N. distans*, are relatively high.

The diatom record from the cores taken within the fjord seems to contain diatom flora which reflects well the living diatom assemblages. In our interpretation this means that the post sedimentary transportation was minimal. A particularly well defined diatom succession is illustrated in core SKPC-01. The benthic forms occur throughout the entire core, their highest abundances are found in the lowermost part of the marine section, which was deposited after the morphological threshold separating the fjord from the ocean was inundated (Witon and Witkowski, 2003). Abundant occurrence of benthic diatoms amongst which taxa with an epiphytic mode of life occur (e.g., *C. costata*, *G. angulosa* var. *islandica*, *R. minutum*; Edsbacke, 1968; Kuylenstierna, 1989–1990; Snoeijis, 1994; Witkowski, unpublished observations), may be interpreted as an indication that the sediment was deposited with the bottom of the fjord covered by macrophytes, enabling the development of epiphytic taxa. During the sedimentation of the DAZ-2b deposits in core SKPC-01 a distinct decrease in epiphytes is observed and in *O. aurita* in particular (Fig. 7). This is associated with distinct dominance of *P. sulcata*, which could be indicative of increased lateral transport and stronger wind factor. In our interpretation, increased current velocities might have resulted in higher turbidity and reduced light intensity by high sediment resuspension, which caused a decrease in macrophyte cover. The currents were apparently not too strong, since the species richness does not show too strong impact of pronounced sorting and removal of epiphytic forms to other sites. Apparently, the oceanographic conditions favouring development of macrophytes and epiphytic diatoms were reestablished for a short period, evidenced by the

appearance of the taxa in the uppermost part of DAZ-2b and lowermost part of DAZ-3b. However, higher up in the core most of them disappeared. This change is dated to ca. 2600 cal. yr BP and is also observed (but less clearly) in core LINK-1 (Fig. 6).

The freshwater diatom flora that occurred between 1200 and 700 cal. yr BP in all four cores (Fig. 4) suggests markedly increased freshwater discharge into the fjord. This suggests that during this time much higher precipitation occurred. This period represents the Medieval Warm Period (MWP), which coincides with the first human settlements on the Faeroe Islands (Hannon et al., 1998; Arge, 1991). Enhanced cyclone activity with associated higher local precipitation thus characterized the MWP on the Faeroe Islands. Large-scale increased atmospheric instability over the (northern) North Atlantic may have been a typical feature of the MWP, as indications for such a regime have recently also been found in South Greenland fjords (e.g., Lassen et al., 2004). Thus, increased snow drift and melt-water runoff from land, in addition to human-induced changes in onshore vegetation and associated nutrient discharge into the fjord played a major role for the increase in the freshwater flora in the Skalafjord. The taxa indicative of increased freshwater runoff belong to the genera of *Eunotia*, *Epithemia*, *Cymbella*, and *Tabellaria*. They were present permanently but in very low abundances. Interesting fact in this respect is also the increased relative abundance of freshwater diatoms and of *A. normanii* in particular in core SKPC-08. This species is believed to be an indicator of eutrophicated waters and belongs nowadays to the group of planktonic taxa with a worldwide distribution. *A. normanii* has recently migrated around the world from being a more restricted diatom (Hasle and Syvertsen, 1996; Witkowski et al., 2000; Garcia-Rodriguez et al., 2002). Here we interpret the presence of this species as an indicator of increasing trophicity, most probably related to human settlement and associated introduction of cattle on the Faeroe Islands. The first human colonisation on the Faeroes has been dated to 1200 cal. yr BP (Arge, 1991; Hannon et al., 1998). In addition, wind-induced mixing of surface waters, as may be expected in case of enhanced cyclone activity, may further have favoured nutrient availability in the euphotic zone.

The MLFA suggests that the fossil diatom record in LINK-1 was related to change in the hydrographic regime of the Faeroe Islands area during the past 4900 years. The investigated time period is divided into three stages characterized by prevalence of different water masses in the fjord. The time intervals between 4900–3000 and 1500–0 cal. yr BP are

interpreted to be marked by inflow of relatively cold water masses and the interval 3000–1500 cal. yr BP by inflow of warmer water masses. In the MLFA the diatom species are divided into factors based on their relations to the environmental variables. Two factors were distinguished: Factor 1 is suggested to represent an indicator of a warmer water ( $\sim 6$  °C) diatom assemblage, and Factor 2 may be an indicator of a colder water (less than 6 °C) diatom assemblage. The critical temperature of 6 °C was assumed based on temperature differences between the water masses around the Faeroes.

There is a slightly discrepancy between the results of MLFA and DAZ's. This situation is caused by strong domination of the species *P. sulcata*. However, its domination does not affect the pattern shown by MLFA.

The ecological preferences of many marine diatom taxa are not well known, but a clue as to the pattern shown by Factor 1 may be provided by previous inferences concerning indicator species for different water masses. For example, two of the species contributing to Factor 1, *T. nitzschioides* and *T. angulata*, are known, to be adapted to relatively high water temperature and salinity (Koç Karpuz and Schrader, 1990). *T. nitzschioides* and *T. angulata* are widespread neritic species, often found in great numbers in the North Sea, and they are common in the North Atlantic and English Channel (Hendey, 1964). Hasle and Syvertsen (1996) described these species as cosmopolitan species. *T. nitzschioides* is one of the dominant species in an assemblage found where the warm and high-saline North Atlantic Water flows into the Skagerrak (Jiang, 1996). It is also one of the chief constituents of the relatively warm Norwegian–Atlantic Current assemblage in the Nordic Seas (Koç Karpuz and Schrader, 1990). In modern surface sediments, *T. nitzschioides* is found most abundantly south and southwest of Iceland, where the warm Irminger Current flows, and it reaches abundances of about 5% on the present north Icelandic shelf (Jiang et al., 2001). *P. sulcata*, which in this factor displays an inverse relationship to *T. nitzschioides* and *T. angulata*, is a cosmopolitan species (Hasle and Syvertsen, 1996). It is very common along the southeastern shores of the North Sea (Hendey, 1964). Around Iceland, it is found at relative shallow water depths with relatively high SST (Jiang et al., 2001). This species could be also indicative of increased lateral transport, which makes an interpretation somewhat difficult. Subsequently, the contributions of *T. nitzschioides* and *T. angulata* to this factor suggest that it represents an index of the influence of the Norwegian–Atlantic Current in the Skalafjord. At times

of a more pronounced influence of Norwegian–Atlantic Current the benthic taxa also contributing to this factor (*P. sulcata*, *N. distans* and *G. angulosa* var. *islandica*) decreased in relative abundance, whereas they were more important components of the flora at times of lesser influence of the Norwegian–Atlantic Current. *R. hebetata* is a species contributing to Factor 2 that is found in the northern cold-water region (Hasle and Syvertsen, 1996). According to Koç Karpuz and Schrader (1990) *R. hebetata* belongs to the Arctic–Norwegian Water Mixing. It is a mixture between Arctic and Atlantic waters, and this water mass is located northeast and southwest of Iceland. Jiang et al. (2001) recorded this species in sediments from the Iceland coast as an indicator of Modified Polar Water of the East Iceland Current. A high number of *R. hebetata* was observed by Smayda (1958) around Jan Mayen at a surface water temperature of 1.5 °C. High occurrence of this species could suggest an eastward fluctuation of the Jan Mayen Current (Kohly, 1998), which suggests that *R. hebetata* could be an indicator of Arctic–Norwegian Water Mixing. The ecological requirements of *R. minutum* are very poorly known, but in our study this species is suggested to represent an indicator of relatively warm water masses flowing into the Skalafjord.

Based on Koç Karpuz and Schrader (1990) the diatom assemblage in the first factor is interpreted as a Norwegian–Atlantic Current (NAC) assemblage and the second factor as an Arctic–Norwegian Water Mixing (ANWM) assemblage. Between 4900 and 3200 cal. yr BP the increase in *R. hebetata* in Factor 2 suggests that during this time interval a cold Arctic–Norwegian Water Mixing could have flown into the Skalafjord, or at least be a part of turbulent mixing of the water column. This episode is comparable with foraminifer and diatom data from the Icelandic Shelf presented by Jiang et al. (2002) and Eiriksson et al. (2000). Based on diatoms Koç et al. (1993) suggested an influence of ANWM with minor influence of Arctic Water on the Iceland Plateau between 5400 and 2500 cal. yr BP, and in the SE Norwegian Sea she recognized a climatic deterioration between 5000 and 3800 cal. yr BP, which is correlated to the Neoglacial cooling recorded in the Scandinavian landscape. Warmer Atlantic waters moved to the southern central part of the Greenland–Iceland–Norwegian Seas, and colder Arctic water masses had a larger influence on the Greenland basin. The East Greenland Current and associated East Iceland Current, which flows further east towards the area north of the Faeroe Islands, is stronger than at 7000 cal. yr BP (Koç et al., 1993).

Between 3200 and 1700 cal. yr BP the influence of the cold ANWM assemblage in Skalafjord drastically decreased. Factor 1 scores, which are indicative of fluctuations in the warm water diatom assemblage (NAC) remain at the same level. The impact of ANWM (Factor 2) is generally much weaker during this time interval, but the scores show strong short-time fluctuations. In our interpretation the diatom flora of this interval (e.g., enrichment of *P. sulcata*, and disappearance *O. aurita*) corresponds to a strongly stratified water-column and the mixing of predominant NAC and ANWM assemblages. This is particularly evident from the absence of *R. hebetata* and presence of *T. nitzschioides* and *T. angulata*. Jiang et al. (2002) recorded relatively warm conditions around Iceland between 3200 and 2400 cal. yr BP, which were interrupted by some periods of gradual cooling of water temperatures. The findings of the present study are also supported by sea surface temperature data from the Norwegian Sea and Reykjanes Ridge south of Iceland that show generally warmer conditions starting after 4000 cal. yr BP which lasted until about 2000 cal. yr BP (Moros et al., 2004). Thus, a clear link appears to exist between hydrographic changes in Skalafjord and variations in large-scale North Atlantic circulation.

After 1700 cal. yr BP the strength of the inflow of warm Norwegian Atlantic waters into the Faeroe Islands was reduced, and the impact of the cold Arctic–Norwegian Water Mixing assemblage was gradually increasing. However, during the period 1200 and 500 cal. yr BP withdrawal of Norwegian Atlantic waters is much less distinct and is characterized by several distinct peaks. This phenomenon would correspond to the “Medieval Warm Period”. The appearance of a few pronounced peaks in Factor 2 scores at ca. 300 cal. yr BP shows stronger impact of cold ANWM and in our opinion this reflects the circulation pattern of the “Little Ice Age”.

## 5. Conclusions

Diatom records from the Faeroe Islands reflect changes in the hydrographic regime of the area during the last 5400 cal. yr. A maximum-likelihood factor analysis (MLFA) based on the 11 most abundant species in core Link-1 shows that a two-factor solution represents the optimum factor model. The first factor is interpreted as a Norwegian–Atlantic Current (NAC) assemblage and the second factor as an Arctic–Norwegian Water Mixing (ANWM) assemblage. The investigated time period is divided into three stages

characterized by prevalence of different water masses in the fjord. The time intervals between 5400–3000 and 1500–0 cal. yr BP are interpreted to be marked by inflow of relatively cold water masses (ANWM) and the stage 3000–1500 cal. yr BP by inflow of warmer water masses (NAC). Diatom analyzes in different parts of the fjord revealed differences in diatom concentrations and assemblages between the inner and outer parts of the fjord. The assemblages in the sediments showed reduced diatom concentration and abundance of lightly silicified taxa towards the mouth of the fjord. Bottom currents at the mouth to the Skalafjord are strong and play a major role in transportation and redeposition of diatom valves. High content of *P. sulcata* is partly a result of redeposition and enrichment of the sediment by lateral transport. The diatom record from the inner part of the fjord represents a more natural distribution. Abundant occurrence of epiphytic diatoms implies that the sediment was deposited with the bottom of the fjord covered by macrophytes, enabling the development of epiphytic taxa. The diatom assemblage of the freshwater flora that occurred between 1200 and 700 cal. yr BP suggests significant freshwater discharge into the fjord. Increased precipitation is suggested to be related to enhanced North Atlantic cyclone activity which may be a typical feature of the Medieval Warm Period. High abundance of *A. normanii* suggests that trophy increased, which is most probably related to human settlement on the Faeroe Islands.

### Acknowledgements

We thank Tine Rasmussen, The University Center in Svalbard for supplying the samples and AMS C-14 dates for core LINK-1. The LINK project has been funded by the Danish Natural Science Research Council under the North Atlantic Programme (Project LINK). The master and crew of the *R/V Skagerak* and *R/V Dana* are thanked for their assistance with the coring work at sea during the 1995 and 2000 cruise (LINK core), respectively. We express our gratitude to Hui Jiang for discussions of the results of the factor analysis.

### Appendix A

Taxonomic list of species identified in cores LINK-1, SKPC-01, SKPC-08, and SKPC-10 from the Faeroe Islands.

### MARINE and BRACKISH

Diatom species	LINK 1	SKPC-01	SKPC-08	SKPC-10
<i>Achnanthes brevipes</i> C.A. Agardh		X		
<i>Achnanthes groenlandica</i> (Cleve) Grunow	X	X		
<i>Achnanthes pseudogroenlandica</i> Hendey	X			
<i>Achnanthes parvula</i> Kützing		X		X
<i>Achnanthidium minutissimum</i> (Kützing) Czamecki				X
<i>Actinocyclus circellus</i> Watkins			X	X
<i>Actinocyclus curvatus</i> Janisch in A. Schmidt				X
<i>Actinocyclus normanii</i> Hustedt			X	
<i>Actinoptychus senarius</i> (Ehrenberg) Ehrenberg	X	X	X	X
<i>Amphora granulata</i> Gregory				X
<i>Amphora cf. helensis</i> Giffen	X	X		
<i>Amphora marina</i> W. Smith		X		X
<i>Amphora proteoides</i> Hustedt		X		
<i>Amphora wiseii</i> (Salah) Simonsen			X	X
<i>Bacterosira bathyomphala</i> (Cleve) Syvertsen and Hasle		X		X
<i>Biremis ambigua</i> (Cleve) D.G. Mann				X
<i>Caloneis bacillum</i> (Grunow) Cleve			X	
<i>Caloneis elongata</i> (Grunow) Cleve			X	
<i>Caloneis westii</i> (W. Smith) Hendey				X
<i>Campylodiscus clypeus</i> Ehrenberg		X		
<i>Campylodiscus fastuosus</i> Ehrenberg		X		X
<i>Campylodiscus thuretii</i> Brébisson		X		
<i>Cocconeis californica</i> Grunow in Van Heurck		X		
<i>Cocconeis carminata</i> Cholnoky			X	
<i>Cocconeis costata</i> Gregory	X	X	X	X
<i>Cocconeis decipiens</i> Cleve		X	X	

<i>Cocconeis dirupta</i> Gregory			X	X	<i>Diploneis incurvata</i> fo. <i>stricta</i> Hustedt		X		
<i>Cocconeis discrepans</i> A. Schmidt				X	<i>Diploneis interrupta</i> (Kützing) Cleve			X	X
<i>Cocconeis distans</i> Gregory				X	<i>Diploneis litoralis</i> (Donkin) Cleve		X		X
<i>Cocconeis guttata</i> Hustedt		X			<i>Diploneis mirabilis</i> König		X		
<i>Cocconeis irregularis</i> (Schulz) Witkowski	X	X			<i>Diploneis notabilis</i> (Greville) Cleve	X	X	X	X
<i>Cocconeis krammeri</i> Lange-Bertalot and Metzeltin	X			X	<i>Diploneis pneumatica</i> S.J.M. Droop		X		
<i>Cocconeis pellucida</i> Grunow ex Hantzsch in Rabenhorst	X				<i>Diploneis sejuncta</i> (A. Schmidt) Jørgensen	X	X		
<i>Cocconeis peltoides</i> Hustedt		X			<i>Diploneis smithii</i> (Brebisson) Cleve		X	X	
<i>Cocconeis pinnata</i> Gregory ex Greville		X	X	X	<i>Diploneis solea</i> S.J.M. Droop				X
<i>Cocconeis pseudomarginata</i> Gregory	X	X	X	X	<i>Diploneis stroemii</i> Hustedt		X		
<i>Cocconeis scutellum</i> var. <i>parva</i> Grunow	X	X	X	X	<i>Diploneis vacillans</i> var. <i>renitens</i> A. Schmidt	X	X		X
<i>Cocconeis scutellum</i> var. <i>scutellum</i> Ehrenberg	X	X	X	X	<i>Diploneis vacillans</i> var. <i>vacillans</i> (A. Schmidt) Cleve	X	X		
<i>Cocconeis speciosa</i> Gregory		X		X	<i>Ehrenbergiulva</i> <i>granulosa</i> (Grunow) Witkowski, Lange-Bertalot and Metzeltin	X			
<i>Cosinodiscus marginatus</i> Ehrenberg	X				<i>Fallacia forcipata</i> (Greville) Stickle and D.G. Mann	X		X	X
<i>Cosinodiscus radiatus</i> Ehrenberg			X	X	<i>Fallacia marnieri</i> (Manguin) Witkowski, Lange-Bertalot and Metzeltin				X
<i>Delphineis surirella</i> (Ehrenberg) Andrews			X		<i>Fallacia subforcipata</i> (Hustedt) D.G. Mann				X
<i>Dimeregramma dubium</i> (Grunow) Grunow in Van Heurck	X				<i>Flagilaria investiens</i> (W. Smith) Cleve–Euler	X	X		
<i>Dimeregramma</i> cf. <i>fulvum</i> (Gregory) Ralfs in Pritchard	X	X	X		<i>Flagilaria martyi</i> mo. <i>grandis</i> Witkowski and Lange-Bertalot	X	X		
<i>Dimeregramma</i> <i>marinum</i> (Gregory) Ralfs in Pritchard	X	X	X		<i>Glyphodesmis distans</i> (Gregory) Grunow in Van Heurck	X		X	
<i>Dimeregramma minor</i> (Gregory) Ralfs in Pritchard			X	X	<i>Gomphonemopsis</i> <i>litoralis</i> (Hendey) Medlin		X		
<i>Diploneis bomboides</i> (A. Schmidt) Cleve	X				<i>Gomphonemopsis</i> <i>obscurum</i> (Krasske) Lange-Bertalot	X	X		
<i>Diploneis bombus</i> Ehrenberg		X			<i>Grammatophora</i> <i>angulosa</i> var. <i>islandica</i> (Ehrenberg) Grunow	X	X	X	X
<i>Diploneis crabro</i> Ehrenberg	X				<i>Grammatophora</i> <i>arcuata</i> Ehrenberg	X	X	X	X
<i>Diploneis dimorpha</i> Hustedt	X								
<i>Diploneis fusca</i> (Gregory) Cleve	X	X							
<i>Diploneis incurvata</i> var. <i>dubia</i> Hustedt		X		X					
<i>Diploneis incurvata</i> var. <i>incurvata</i> (Gregory) Cleve				X					

(continued on next page)

Diatom species	LINK 1	SKPC-01	SKPC-08	SKPC-10					
<i>Grammatophora hamulifera</i> Kützing			X	X	<i>Nitzschia rorida</i> Giffen		X		
<i>Grammatophora macilenta</i> W. Smith			X	X	<i>Odontella aurita</i> (Lyngbye) C.A. Agardh	X	X	X	X
<i>Grammatophora marina</i> (Lyngbye) Kützing		X	X	X	<i>Opephora marina</i> (Gregory) Petit	X	X	X	X
<i>Grammatophora maxima</i> Grunow				X	<i>Opephora pacifica</i> (Grunow) Petit			X	
<i>Grammatophora oceanica</i> (Ehrenberg) Grunow		X	X	X	<i>Paralia sulcata</i> (Ehrenberg) Cleve	X	X	X	X
<i>Grammatophora serpentina</i> (Ralfs) Ehrenberg	X	X	X	X	<i>Parlibellus berkeleyi</i> (Kützing) Cox		X		
<i>Grammatophora subtilissima</i> Bailey			X		<i>Pinnularia quadratarea</i> (A. Schmidt) Cleve			X	X
<i>Hippodonta linearis</i> (Østrup) Lange-Bertalot, Metzeltin and Witkowski	X		X		<i>Plagiogramma staurophorum</i> (Gregory) Heiberg	X	X	X	X
<i>Licmophora gracilis</i> (Ehrenberg) Grunow				X	<i>Planothidium delicatulum</i> (Kützing) Round and Bukhtiyarova				
<i>Lyrella abrupta</i> (Gregory) D.G. Mann	X				<i>Planothidium lilljeborgei</i> (Grunow) Witkowski, Lange-Bertalot and Metzeltin	X			x
<i>Lyrella cf. amphoroides</i> D.G. Mann	X	X			<i>Pleurosigma normanii</i> Ralfs in Pritchard	X	X		X
<i>Lyrella hennedyi</i> (Hennedyi) Stickle and D.G. Mann	X				<i>Porosira glacialis</i> (Grunow) Jørgensen			X	
<i>Lyrella lyra</i> (Ehrenberg) Karayeva		X			<i>Psammodiscus nitidus</i> (Gregory) Round and D.G. Mann	X			
<i>Lyrella spectabilis</i> (Gregory) D.G. Mann			X	X	<i>Pseudogomphonema plinskii</i> Witkowski, Metzeltin and Lange-Bertalot	X	X		
<i>Mastogloia pumila</i> (Grunow) Cleve			X		<i>Raphoneis amphiceros</i> (Ehrenberg) Ehrenberg	X			
<i>Melosira lineata</i> (Dillwyn) C.A. Agardh			X	X	<i>Rhabdonema adriaticum</i> Kützing	X			
<i>Melosira moniliformis</i> (O.F. Müller) C.A. Agardh			X	X	<i>Rhabdonema arcuatum</i> (C.A. Agardh) Kützing	X	X	X	X
<i>Navicula distans</i> (W. Smith) A. Schmidt	X	X	X	X	<i>Rhabdonema minutum</i> Kützing	X	X	X	
<i>Navicula diversistriata</i> Hustedt		X			<i>Rhizosolenia borealis</i> Sundström	X	X	X	X
<i>Navicula normalis</i> Hustedt		X			<i>Rhizosolenia hebetata</i> Bailey fo. <i>hebetata</i>	X	X	X	X
<i>Navicula palpebralis</i> Brebisson ex W. Smith			X		<i>Rhizosolenia hebetata</i> fo. <i>semispina</i> (Hensen) Gran	X	X	X	X
<i>Navicula cf. vara</i> Hustedt	X	X		X	<i>Rhoicosphenia marina</i> (W. Smith) M. Schmidt		X		
<i>Nitzschia coarctata</i> Grunow	X	X	X	X	<i>Rhopalodia acuminata</i> Krammer	X	X	X	X
<i>Nitzschia compressa</i> (Bailey) Boyer			X	X					
<i>Nitzschia ligowskii</i> Witkowski, Lange-Bertalot, Kociolek and Brzezinska		X							
<i>Nitzschia pusilla</i> Grunow		X							

<i>Rhopalodia gibba</i> (Ehrenberg) O. Müller	X		X	
<i>Rhopalodia pacifica</i> Krammer	X			
<i>Surirella birostrata</i> Hustedt	X			
<i>Surirella linearis</i> W. Smith			X	
<i>Synedra tabulata</i> (C.A. Agardh) Kützing		X		
<i>Tabularia ktenoeoides</i> Kuylenstierna	X	X		
<i>Thalassionema nitzschioides</i> (Grun.) Grun. ex Hustedt	X	X	X	X
<i>Thalassionema pseudonitzschioides</i> (Schuette and Schrader) Hasle	X	X		X
<i>Thalassiosira angulata</i> (Gregory) Hasle	X			
<i>Thalassiosira antarctica</i> Comber	X	X	X	X
<i>Thalassiosira baltica</i> (Grun.) Ostenfeld	X	X	X	X
<i>Thalassiosira decipiens</i> (Grun.) Jørgensen		X	X	
<i>Thalassiosira eccentrica</i> (Ehrenberg) Cleve	X	X	X	
<i>Thalassiosira hyalina</i> (Grun.) Gran				X
<i>Thalassiosira levanderi</i> Van Goor	X			X
<i>Thalassiosira nordenskiöldii</i> Cleve	X	X	X	X
<i>Thalassiosira oestrupii</i> (Ostenfeld) Hasle			X	
<i>Thalassiosira pacifica</i> Gran and Angst	X	X	X	X
<i>Trachyneis aspera</i> (Ehrenberg) Cleve	X	X	X	

**FRESHWATER**

Diatom species	LINK 1	SKPC-01	SKPC-08	SKPC-10
<i>Amphora copulata</i> (Kütz.) Schoeman and Archibald		X	X	
<i>Amphora pediculus</i> (Kützing) Grunow	X	X	X	X
<i>Amphora veneta</i> Kützing		X		X
<i>Aulacoseira subarctica</i> (O. Müller) Haworth		X		
<i>Aulacoseira valida</i> (Grunow) Krammer		X		
<i>Brachysira brebissonii</i> Ross				X
<i>Brachysira vitrea</i> (Grunow) Ross			X	

<i>Caloneis undulata</i> (Gregory) Krammer		X		
<i>Cocconeis placentula</i> Ehrenberg		X		X
<i>Cocconema cymbiforme</i> (Kützing) Ehrenberg				X
<i>Cyclotella ocellata</i> Pantocsek		X	X	
<i>Cymbella affinis</i> Kützing				X
<i>Diademesmis perpusilla</i> (Grunow) Lange-Bertalot		X	X	
<i>Diatoma mesodon</i> (Ehrenberg) Kützing			X	X
<i>Diatoma moniliformis</i> Kützing				X
<i>Diatomella balfouriana</i> Greville		X		X
<i>Diploneis ovalis</i> (Hilse) Cleve		X		X
<i>Encyonema silesiacum</i> (Bleisch) D.G. Mann		X	X	X
<i>Epithemia adnata</i> (Kützing) Brebisson	X	X	X	
<i>Epithemia sorex</i> Kützing				X
<i>Eunotia arcus</i> Ehrenberg		X	X	
<i>Eunotia bilunaris</i> (Ehrenberg) Mills		X	X	
<i>Eunotia curtagrunowii</i> Nörpel-Schempp and Lange-Bertalot				X
<i>Eunotia glacialis</i> Meister				X
<i>Eunotia implicata</i> Nörpel-Schempp, Lange-Bertalot and Alles	X			
<i>Eunotia incisa</i> Gregory	X	X	X	X
<i>Eunotia pseudopectinalis</i> (Brebisson) Kützing		X	X	
<i>Gomphonema affine</i> Kützing		X		
<i>Navicula radiosa</i> Kützing		X	X	X
<i>Nitzschia angustata</i> Grunow		X		X
<i>Pinnularia notabilis</i> Krammer		X		X
<i>Stauwoforma exiguiformis</i> (Grunow) Flower, Jones and Round	X	X	X	X
<i>Stauroneis neohyalina</i> Lange-Bertalot and Krammer	X			
<i>Tabellaria fenestrata</i> (Lyngbye) Kützing		X	X	
<i>Tabellaria flocculosa</i> (Roth) Kützing	X	X	X	X

## References

- Aitchison, J., 1986. The Statistical Analysis of Compositional Data. Chapman & Hall, New York. 416 pp.
- Andrews, J.T., Giraudeau, J., 2003. Multi-proxy records showing significant Holocene environmental variability: the inner N. Iceland shelf (Hunafloi). *Quaternary Science Reviews* 22, 175–193.
- Arge, S.V., 1991. The Landnam in the Faroes. *Arctic Anthropology* 28, 101–120.
- Baldauf, J.G., 1981. Diatom analysis of late Quaternary sediments from the Navarin basin province, Bering Sea. *Seafloor Geologic Hazards, Sedimentology, and Bathymetry: Navarin Basin Province, Northwestern Bering Sea*. United States Geological Survey Open-File Report, vol. 81-1217, pp. 100–113.
- Birks, C.J.A., Koc, N., 2002. A high-resolution diatom record of late-Quaternary sea-surface temperatures and oceanographic conditions from the eastern Norwegian Sea. *Boreas* 31, 323–344.
- Brun, J., 1901. Diatomees d'eau douce de l'île Jan Mayen et de la cote du Groenland, recoltées par l'expédition suédoise de 1899. *Kungliga Vetenskaps Svenska Akademiens Handlingar* 26, 1–22.
- Calvo, E., Grimalt, J., Jansen, E., 2002. High resolution  $U_{37}^k$  sea surface temperature reconstruction in the Norwegian Sea during the Holocene. *Quaternary Science Reviews* 21, 1385–1394.
- Cleve, P.T., 1873. On diatoms from the Arctic Sea. *Kungliga Vetenskaps Svenska Akademiens Handlingar* 1, 1–28.
- Cleve, P.T., 1896. Diatoms from Baffin Bay and Davis Strait. *Kungliga Vetenskaps Svenska Akademiens Handlingar* 22 (III), 4.
- Cleve, P.T., 1898. The plankton of the North Sea, the English Channel and the Skagerrak in 1898. *Kungliga Vetenskaps Svenska Akademiens Handlingar* 32, 1–53.
- Cleve, P.T., 1900. Notes on some Atlantic plankton organisms. *Kungliga Vetenskaps Svenska Akademiens Handlingar* 34, 20.
- Cleve, P.T., Grunow, A., 1880. Beiträge zur Kenntnis der arktischen Diatomeen. *Kungliga Vetenskaps Svenska Akademiens Handlingar* 17, 1–121.
- Cremer, H., 1999. Distribution patterns of diatom surface sediment assemblages in the Laptev Sea (Arctic Ocean). *Marine Micropaleontology* 38, 39–67.
- Edsbagge, H., 1968. Zur Ökologie der Marinen angehefteten Diatomeen. *Botanica Gothoburgensia* 6, 1–153.
- Efron, B., Tibshirani, R.J., 1993. An Introduction to the Bootstrap. Chapman and Hall (Eds). New York, pp. 1–436.
- Eiriksson, J., Knudsen, K.L., Hafliðason, H., Heinemeier, J., 2000. Chronology of late Holocene climatic events in the northern North Atlantic based on AMS  $^{14}C$  dates and tephra markers from the volcano Hekla, Iceland. *Journal of Quaternary Science* 15, 573–580.
- Enell, M., 1996. Environmental impact of nutrients from Nordic fish farming. *Environmental Pollution* 93, 105–106.
- García-Rodríguez, F., Witkowski, A., 2003. Inferring sea level variation from relative percentages of *Pseudopodosira kosugii* in Rocha Lagoon, SE Uruguay. *Diatom Research* 18, 49–59.
- García-Rodríguez, F., Mazzeo, N., Sprechmann, P., Metzeltin, D., Sosa, F., Treutler, H.C., Renom, M., Scharf, B., Gaucher, C., 2002. Paleolimnological assessment of human impacts in Lake Blanca, SE Uruguay. *Journal of Paleolimnology* 28, 457–468.
- Gran, H.H., 1900. Diatomaceae from the icefloes and plankton of the Arctic Ocean. The Norwegian North Polar Expedition 1893–6. *Scientific Results*, vol. 4.
- Håkansson, H., Ross, R., 1984. Proposals to designate conserved types for *Cymbella* and *Cyclotella*, and to conserve *Rhopalodia* against *Pyxidicula* (all Bacillariophyceae). *Taxon* 33, 525–531.
- Hannon, G.E., Bradshaw, R., 2000. Impacts and timing of the first human settlement on vegetation of the Faroe Islands. *Quaternary Research* 54, 404–413.
- Hannon, G.E., Hermanns-Auðardóttir, M., Wastegård, S., 1998. Human impact at Tjørnuvík on the Faroe Islands. *Fróðskaparrit* 46, 215–228.
- Hansen, B., Østerhus, S., 2000. North Atlantic–Nordic Seas exchanges. *Progress in Oceanography* 45, 109–208.
- Hansen, B., Kristiansen, R., Lastein, L., 1990. Hydrografískar kanningar á føroysku gáttarfrøðnum. *Fiskirannsóknir* 6, 75–98.
- Hasle, G.R., 1978. Some *Thalassiosira* species with one central process (Bacillariophyceae). *Norwegian Journal of Botany* 25, 77–110.
- Hasle, G.R., Syvertsen, E.E., 1996. Marine diatoms. In: Tomas, C.R. (Ed.), *Identifying Marine Phytoplankton*. Academic Press, California, pp. 5–385.
- Hendey, N.I., 1964. An introductory account of the smaller algae of British coastal waters. Part V. Bacillariophyceae (Diatoms). *Fishery Investigations Series*, vol. 4. Koeltz Scientific Books Koenigstein, London, pp. 1–317.
- Hendrickson, A.E., White, P.O., 1964. Promax: a quick method for rotation to oblique simple structure. *British Journal of Statistical Psychology* 17, 65–70.
- Jiang, H., 1996. Diatoms from the surface sediments of the Skagerrak and Kattegat and their relationship to the spatial changes of environmental variables. *Journal of Biogeography* 23, 129–137.
- Jiang, H., Seidenkrantz, M.S., Knudsen, K.L., Eriksson, J., 2001. Diatom surface sediment assemblages around Iceland and their relationships to oceanic environmental variables. *Marine Micro-paleontology* 41, 73–96.
- Jiang, H., Seidenkrantz, M.S., Knudsen, K.L., Eriksson, J., 2002. Late-Holocene summer sea-surface temperatures based on diatom record from the north Icelandic shelf. *The Holocene* 12, 137–146.
- Juggins, S., 1992. Diatoms in the Thames Estuary, England: ecology, paleoecology, and salinity transfer function. *Bibliotheca Diatomologica*, vol. 25. J. Cramer, Stuttgart, Germany, pp. 1–216.
- Juul, M., 1992. Den Holocæne udvikling i Skålafjord, Færøerne. Student thesis, Institute of Geology, Aarhus University, Denmark.
- Koç Karpuz, N., Jansen, E., 1992. A high-resolution diatom record of the last deglaciation from the SE Norwegian Sea: documentation of rapid climatic changes. *Paleoceanography* 7, 499–520.
- Koç Karpuz, N., Schrader, H., 1990. Surface sediment diatom distribution and Holocene paleotemperature variations in the Greenland, Iceland and Norwegian Sea. *Paleoceanography* 5, 557–580.
- Koç, N., Jansen, E., Hafliðason, H., 1993. Paleoceanographic reconstructions of surface ocean conditions in the Greenland, Iceland and Norwegian Seas through the last 14 ka based on diatoms. *Quaternary Sciences Reviews* 12, 115–140.
- Kohly, A., 1998. Diatom flux and species composition in the Greenland Sea and the Norwegian Sea in 1991–1992. *Marine Geology* 145, 293–312.
- Kuijpers, A., Andersen, M.S., Kenyon, N.H., Kunzendorf, H., Van Weering, T.C.E., 1998a. Quaternary sedimentation and Norwegian Sea overflow pathways around Bill Bailey Bank, northeastern Atlantic. *Marine Geology* 152, 101–127.
- Kuijpers, A., Troelstra, S.R., Oppo, D., Wisse, M., Heier Nielsen, S., Van Weering, T.C.E., 1998b. Norwegian Sea overflow variability

- and NE Atlantic surface hydrography during the past 150,000 years. *Marine Geology* 152, 75–99.
- Kuijpers, A., Hansen, B., Hühnerbach, V., Larsen, B., Nielsen, T., Werner, F., 2002. Norwegian Sea overflow through the Faroe–Shetland gateway as documented by its bedforms. *Marine Geology* 188, 147–164.
- Kuylenstierna, M., 1989–1990. Benthic Algal Vegetation in the Nordre Älv Estuary, vol. 1. PhD dissertation. Department of Marine Botany. Göteborg University, Sweden.
- Lagerstedt, N.G.W., 1873. Sötavattens-Diatomeer fran Spetsbergen och Beeren Einland. *Kungliga Vetenskaps Svenska Akademiens Handlingar* 1, 1–52.
- Larsen, B., 1991. Maringeologiske målinger ved Faerøerne, 19.–25. Juni 1991. DGU Datadokumentation, vol. 3. Geological Survey of Denmark, Copenhagen, pp. 1–6.
- Lassen, S.J., Kuijpers, A., Kunzendorf, H., Hoffmann-Wieck, G., Mikkelsen, N., Konradi, P., 2004. Late-Holocene Atlantic bottom water variability in Igaliku Fjord, south Greenland, reconstructed from foraminifera faunas. *The Holocene* 14 (2), 165–171.
- Lawley, D.N., Maxwell, A.E., 1971. Factor Analysis as a Statistical Method, 2nd ed. Butterworths, London. 153 pp.
- Lynghye, H.C., 1819. Tentamen hydrophytologiae Danicae continens omnia hydrophyta cryptogama Daniae, Holsatiae, Foeroeae, Islandiae, Groenlandiae hucusque cognita, systematicae disposita, descripta et iconibus illustrata, adjectis simul speciebus Norvegicis. Schultz, Hafniae, Copenhagen.
- Metzeltin, D., Witkowski, A., 1996. Diatomeen der Bären-Insel. In: Lange-Bertalot, H. (Ed.), *Iconografia Diatomologica*, vol. 4. Koeltz Scientific Books Koenigstein, Germany, pp. 1–232.
- Moros, M., Emeis, K., Risebrobakken, B., Snowball, I., Kuijpers, A., McManus, J., Jansen, E., 2004. Sea surface temperatures and ice rafting in the Holocene North Atlantic: climate influences on northern Europe and Greenland. *Quaternary Science Reviews* 23, 2113–2126.
- Nielsen, T., van Weering, T.C.E., 1998. Seismic stratigraphy and sedimentary processes at the Norwegian Sea margin northeast of the Faeroe Islands. *Marine Geology* 152, 141–157.
- Østrup, E., 1895. Marine Diatomæer fra Østgrønland. In: Ryder, C. (Ed.), *Den østrønlandske Expedition, udført i Aarene 1891–92. Meddelelser om Grønland*, vol. 18, pp. 395–476.
- Østrup, E., 1897. Kyst-Diatomeer fra Grønland. *Meddelelser om Grønland* 15, 305–362.
- Polyakova, Y.I., 1994. Peculiarities of diatom thanatocoenoses formation in the sediments of Eurasian Arctic Seas. *Oceanology* 34, 405–414.
- Rasmussen, T.L., Thomsen, E., Labeyrie, L., van Weering, T.C.E., 1996a. Circulation changes in the Faeroe–Shetland Channel correlating with cold events during the last glacial period (58–10 ka). *Geology* 24, 937–940.
- Rasmussen, T.L., Thomsen, E., van Weering, T.C.E., Labeyrie, L., 1996b. Rapid changes in surface and deep water conditions at the Faeroe Margin during the last 58,000 years. *Paleoceanography* 11, 757–771.
- Rasmussen, T.L., Wastegård, S., Kuijpers, A., van Weering, T.C.E., Heinemeier, J., Thomsen, E., 2003. Stratigraphy and distribution of tephra layers in marine sediment cores from the Faeroe Islands, North Atlantic. *Marine Geology* 199, 263–277.
- Reyment, R.A., Jöreskog, K.G., 1993. *Applied Factor Analysis in the Natural Sciences*. Cambridge University Press, Cambridge. 371 pp.
- Risebrobakken, B., Jansen, E., Andersson, C., Mjelde, E., Hevroy, K., 2003. A high-resolution study of Holocene paleoclimatic and paleoceanographic changes in the Nordic Seas. *Paleoceanography* 18, 1017–1031.
- Roncaglia, L., 2004. Palynofacies analysis and organic-walled dinoflagellate cysts as indicators of palaeohydrographic changes: an example from Holocene sediments in Skalafjord, Faeroe Islands. *Marine Micropaleontology* 50, 21–42.
- Schrader, H., 1972. Anlösung und Konservation von Diatomeenschalen beim Absinken am Beispiel des Landsort-Tiefs in der Ostsee. *Nova Hedwigia* 39, 191–216.
- Schrader, H., Gersonde, R., 1978. Diatoms and silicoflagellates. *Utrecht Micropaleontological Bulletin* 17, 129–176.
- Schrader, H., Lindström Swanberg, I., Burckle, L.H., Grønlien, L., 1993a. Diatoms in recent Atlantic (20°S to 70°N latitude) sediments: abundance patterns and what they mean. *Hydrobiologia* 269/270, 129–135.
- Schrader, H., Isrenn, K., Swanberg, N., Paetzel, M., Seathre, T., 1993b. Early Holocene diatom pulse in the Norwegian Sea and its paleoceanographic significance. *Diatom Research* 8, 117–130.
- Smayda, T.J., 1958. Phytoplankton studies around Jan Mayen Island March–April, 1955. *Nytt Magazin for Botanik* 6, 75–96.
- Snoeijs, P.J.M., 1994. Distribution of epiphytic diatom species composition, diversity and biomass on different macroalgal hosts along seasonal and salinity gradients in the Baltic Sea. *Diatom Research* 9, 189–211.
- Stuiver, M., Reimer, P.J., 1993. Extended <sup>14</sup>C data-base and revised calib 3.0 C-14 age calibration program. *Radiocarbon* 35, 215–230.
- Stuiver, M., Reimer, P.J., Bard, E., Beck, J.W., Burr, G.S., Hugen, K., Kromer, B., McCormac, F.G., v.d. Plicht, J., Spurk, M., 1998. INTCAL98 Radiocarbon age calibration 24,000–0 cal. yr. BP. *Radiocarbon* 40, 1041–1083.
- Taylor, J., Dowdeswell, J.A., Kenyon, N.H., Whittington, R.J., van Weering, T.C.E., Mienert, J., 2000. Morphology and Late Quaternary sedimentation on the North Faeroes slope and abyssal plain, North Atlantic. *Marine Geology* 168, 1–24.
- Thomson, G.H., 1951. *The Factorial Analysis of Human Ability*, 5th ed. University of London Press, London. 383 pp.
- van Weering, T.C.E., Nielsen, T., Kenyon, N.H., Akentieva, K., Kuijpers, A.H., 1998. Sediments and sedimentation at the NE Faeroe continental margin; contourites and large-scale sliding. *Marine Geology* 152, 159–176.
- Wastegård, S., 2002. Early to middle Holocene silicic tephra horizons from the Katla volcanic system, Iceland: new results from the Faeroe Islands. *Journal of Quaternary Science* 17, 723–730.
- Wastegård, S., Björck, S., Grauert, M., Hannon, G.E., 2001. The Mjåuvøtn tephra and other Holocene tephra horizons from the Faeroe Islands: a link between the Icelandic source region, the Nordic Seas, and the European continent. *The Holocene* 11, 101–109.
- Witak, M., Wachnicka, A., Kuijpers, A., Troelstra, S., Prins, M.A., Witkowski, A., 2005. Holocene North Atlantic surface circulation and climate variability: evidence from diatom records. *The Holocene* 15, 85–96.
- Witkowski, A., Lange-Bertalot, H., Metzeltin, D., 2000. Diatom Flora of Marine Coasts: I. In: Lange-Bertalot, H. (Ed.), *Iconographia Diatomologica*, vol. 7. A.R.G. Gantner, Germany, pp. 1–905.
- Witon, E., Witkowski, A., 2003. Diatom (Bacillariophyceae) flora of early Holocene freshwater sediments from Skalafjord, Faeroe Islands. *Journal of Micropaleontology* 22, 183–208.
- Zong, Y., Horton, B.P., 1999. Diatom-based tidal-level transfer functions as an aid in reconstructing Quaternary history of sea-level movements in the UK. *Journal of Quaternary Science* 14, 153–167.